

Fast Covariance Estimation for Multivariate Sparse Functional Data

Cai Li^{1,*}, Luo Xiao¹ and Sheng Luo²

¹ North Carolina State University and ²Duke University

*email: cli9@ncsu.edu

September 12, 2022

Abstract

Covariance estimation is essential yet underdeveloped for analyzing multivariate functional data. We propose a fast covariance estimation method for multivariate sparse functional data using bivariate penalized splines. The tensor-product B-spline formulation of the proposed method enables a simple spectral decomposition of the associated covariance operator and explicit expressions of the resulting eigenfunctions as linear combinations of B-spline bases, thereby dramatically facilitating subsequent principal component analysis. We derive a fast algorithm for selecting the smoothing parameters in covariance smoothing using leave-one-subject-out cross-validation. The method is evaluated with extensive numerical studies and applied to an Alzheimer's disease study with multiple longitudinal outcomes.

Keywords: *Bivariate smoothing, Covariance function, Functional principal component analysis, Longitudinal data, Multivariate functional data, Prediction.*

1 Introduction

Functional data analysis (FDA) has been enjoying great successes in many applied fields, e.g., neuroimaging (Reiss and Ogden, 2010; Lindquist, 2012; Goldsmith et al., 2012; Zhu et al., 2012), genetics (Leng and Müller, 2006; Reimherr and Nicolae, 2014, 2016), and wearable computing (Morris et al., 2006; Xiao et al., 2015). Functional principal component analysis (FPCA) conducts dimension reduction on the inherently infinite-dimensional functional data, and thus facilitates subsequent modeling and analysis. Traditionally, functional data are densely observed on a common grid and can be easily connected to multivariate data, although the notation of smoothness distinguishes the former from the latter. In recent years, covariance-based FPCA (Yao et al., 2005) has become a standard approach and has greatly expanded the applicability of functional data methods to irregularly spaced data such as longitudinal data. Various nonparametric methods have now been proposed to estimate the smooth covariance function, e.g., Peng and Paul (2009), Cai and Yuan (2010), Goldsmith et al. (2012) and Xiao et al. (2018).

There has been growing interest in multivariate functional data where multiple functions are observed for each subject. For dense functional data, Ramsay and Silverman (2005, Chapter 8.5) proposed to concatenate multivariate functional data as a single vector and conduct multivariate PCA on the long vectors and Berrendero et al. (2011) repeatedly applied point-wise univariate PCA. For sparse and paired functional data, Zhou et al. (2008) extended the low-rank mixed effects model in James et al. (2000). Chiou et al. (2014) considered normalized multivariate FPCA through standardizing the covariance operator. Petersen and Müller (2016) proposed various metrics for studying cross-covariance between multivariate functional data. More recently, Happ and Greven (2017) introduced a FPCA framework for multivariate functional data defined on different domains.

The interest of the paper is functional principal component analysis for multivariate sparse functional data, where multiple responses are observed at time points that vary from subjects to subjects. There are much fewer works to handle such data. The approach in Zhou et al. (2008) focuses on bivariate functional data and can be extended

to more than two-dimensional functional data, although model selection (e.g., selection of smoothing parameters) can be computationally difficult and convergence of the expectation-maximization estimation algorithm could also be an issue. The local polynomial method in Chiou et al. (2014) can be applied to multivariate sparse functional data, although a major drawback is the selection of multiple bandwidths. Moreover, because the local polynomial method is a local approach, there is no guarantee that the resulting estimates of covariance functions will lead to a properly defined covariance operator. The approach in Happ and Greven (2017) (denoted by mFPCA hereafter) estimates cross-covariances via scores from univariate FPCA and hence can be applied to multivariate sparse functional data. While mFPCA is theoretically sound for dense functional data, it may not capture cross-correlations between functions because scores from univariate FPCA for sparse functional data are biased.

We propose a novel and fast covariance-based FPCA method for multivariate sparse functional data. Note that multiple auto-covariance functions for within-function correlations and cross-covariance functions for between-function correlations have to be estimated. Tensor-product B-splines are employed to approximate the covariance functions and a smoothness penalty as in bivariate penalized splines (Eilers and Marx, 2003) is adopted to avoid overfit. Then the individual estimates of covariance functions will be pooled and refined. The advantages of the new method are multifold. First, the tensor-product B-spline formulation is computationally efficient to handle multivariate sparse functional data. Second, a fast fitting algorithm for selecting the smoothing parameters will be derived, which alleviates the computational burden of conducting leave-one-subject-out cross-validation. Third, the tensor-product B-spline representation of the covariance functions enables a straightforward spectral decomposition of the covariance operator for the multivariate functional data; see Proposition 1. In particular, the eigenfunctions associated with the covariance operator are explicit functions of the B-spline bases. Last but not the least, via a simple truncation step, the refined estimates of the covariance functions lead to a properly defined covariance operator.

Compared to mFPCA, the proposed method does not rely on biased scores from univariate FPCA, which could be a severe problem for sparse functional data, and hence

could better capture the correlations between functions. And an improved correlation estimation will lead to improved subsequent FPCA analysis and curve prediction. The proposed method also compares favorably with the local polynomial method in Chiou et al. (2014) because of the computationally efficient tensor-product spline formulation of the covariance functions and the derived fast algorithm for selecting the smoothing parameters. Moreover, as mentioned above, we shall derive an explicit and easy-to-calculate relationship between the tensor-product spline representation of covariance functions and the associated eigenfunctions/eigenvalues, which greatly facilitates subsequent FPCA analysis.

In addition to FPCA, there are also abundant literatures on models for multivariate functional data with most focusing on dense functional data. For clustering of multivariate functional data, see Zhu et al. (2012); Jacques and Preda (2014); Huang et al. (2014) and Park and Ahn (2017). For regression with multivariate functional responses, see Zhu et al. (2012); Luo and Qi (2017); Li et al. (2017); Wong et al. (2017); Zhu et al. (2017); Kowal et al. (2017) and Qi and Luo (2018). Graphical models for multivariate functional data are studied in Zhu et al. (2016) and Qiao et al. (2017). Works on multivariate functional data include also Chiou and Müller (2014, 2016).

The remainder of the paper proceeds as follows. In Section 2, we present our proposed method. We conduct extensive simulation studies in Section 3 and apply the proposed method to an Alzheimer’s disease study in Section 4. A discussion is given in Section 5. All technical details are enclosed in the Appendix.

2 Methodology

2.1 Fundamentals of Multivariate Functional Principal Component Analysis

Let p be a positive integer and denote by \mathcal{T} a continuous and bounded domain in the real line \mathbb{R} . Consider the Hilbert space $\mathcal{H} : \underbrace{L^2(\mathcal{T}) \times \dots \times L^2(\mathcal{T})}_p$ equipped with the inner product $\langle \cdot, \cdot \rangle_{\mathcal{H}}$ and norm $\| \cdot \|_{\mathcal{H}}$ such that for arbitrary functions $\mathbf{f} =$

$(f^{(1)}, \dots, f^{(p)})^\top$ and $\mathbf{g} = (g^{(1)}, \dots, g^{(p)})^\top$ in \mathcal{H} with each element in $L^2(\mathcal{T})$, $\langle \mathbf{f}, \mathbf{g} \rangle_{\mathcal{H}} = \sum_{k=1}^p \int f^{(k)}(t)g^{(k)}(t)dt$ and $\|\mathbf{f}\|_{\mathcal{H}} = \langle \mathbf{f}, \mathbf{f} \rangle_{\mathcal{H}}^{1/2}$. Let $\{x^{(k)}\}_{k=1, \dots, p}$ be a set of p random functions with each function in $L^2(\mathcal{T})$. Assume that the p -dimensional vector $\mathbf{x}(t) = (x^{(1)}, \dots, x^{(p)})^\top \in \mathbb{R}^p$ has a p -dimensional smooth mean function, $\boldsymbol{\mu}(t) = \mathbb{E}\{\mathbf{x}(t)\} = (\mathbb{E}\{x^{(1)}(t)\}, \dots, \mathbb{E}\{x^{(p)}(t)\})^\top = (\mu^{(1)}(t), \dots, \mu^{(p)}(t))^\top$. Define the covariance function as $\mathbf{C}(s, t) = \mathbb{E}\{(\mathbf{x}(s) - \boldsymbol{\mu}(s))(\mathbf{x}(t) - \boldsymbol{\mu}(t))^\top\} = [C_{kk'}(s, t)]_{1 \leq k, k' \leq p}$ and $C_{kk'}(s, t) = \text{Cov}\{x^{(k)}(s), x^{(k')}(t)\}$. Then the covariance operator $\boldsymbol{\Gamma} : \mathcal{H} \rightarrow \mathcal{H}$ associated with the kernel $\mathbf{C}(s, t)$ can be defined such that for any $\mathbf{f} \in \mathcal{H}$, the k th element of $\boldsymbol{\Gamma}\mathbf{f}$ is given by

$$(\boldsymbol{\Gamma}\mathbf{f})^{(k)}(s) = \langle \mathbf{C}_k(s, \cdot), \mathbf{f} \rangle_{\mathcal{H}} = \sum_{k'=1}^p \int C_{kk'}(s, t) f^{(k')}(t) dt,$$

where $\mathbf{C}_k(s, t) = (C_{k1}(s, t), \dots, C_{kp}(s, t))^\top$. Note that $\boldsymbol{\Gamma}$ is a linear, self-adjoint, compact and non-negative integral operator. By the Hilbert-Schmidt theorem, there exists a set of orthonormal bases $\{\boldsymbol{\Psi}_\ell\}_{\ell \geq 1} \in \mathcal{H}$, $\boldsymbol{\Psi}_\ell = (\Psi_\ell^{(1)}, \dots, \Psi_\ell^{(p)})^\top$, and $\langle \boldsymbol{\Psi}_\ell, \boldsymbol{\Psi}_{\ell'} \rangle_{\mathcal{H}} = \sum_{k=1}^p \int \Psi_\ell^{(k)}(t) \Psi_{\ell'}^{(k)}(t) dt = 1_{\{\ell=\ell'\}}$, such that

$$(\boldsymbol{\Gamma}\boldsymbol{\Psi}_\ell)^{(k)}(s) = \sum_{k'=1}^p \int C_{kk'}(s, t) \Psi_\ell^{(k')}(t) dt = d_\ell \Psi_\ell^{(k)}(s), \quad (1)$$

where d_ℓ is the ℓ th largest eigenvalue corresponding to $\boldsymbol{\Psi}_\ell$. Then the multivariate Mercer's theorem gives

$$\mathbf{C}(s, t) = \sum_{\ell}^{\infty} d_\ell \boldsymbol{\Psi}_\ell(s) \boldsymbol{\Psi}_\ell^\top(t), \quad (2)$$

where $C_{kk'}(s, t) = \sum_{\ell=1}^{\infty} d_\ell \Psi_\ell^{(k)}(s) \Psi_\ell^{(k')}(t)$. As shown in Saporta (1981), $\mathbf{x}(t)$ has the multivariate Karhunen-Loève representation, $\mathbf{x}(t) = \boldsymbol{\mu}(t) + \sum_{\ell=1}^{\infty} \xi_\ell \boldsymbol{\Psi}_\ell(t)$, where $\xi_\ell = \langle \mathbf{x} - \boldsymbol{\mu}, \boldsymbol{\Psi}_\ell \rangle_{\mathcal{H}}$ are the scores with $\mathbb{E}(\xi_\ell) = 0$ and $\mathbb{E}(\xi_\ell \xi_{\ell'}) = d_\ell 1_{\{\ell=\ell'\}}$. The covariance operator $\boldsymbol{\Gamma}$ has the positive semi-definiteness property, i.e, for any $\mathbf{a} = (a_1, \dots, a_p)^\top \in \mathbb{R}^p$, the covariance function of $\mathbf{a}^\top \mathbf{x}$, denoted by $C_{\mathbf{a}}(s, t)$, satisfies that for any sets of time points $(t_1, \dots, t_q) \subset \mathcal{T}$ with an arbitrary positive integer q , the square matrix $[C_{\mathbf{a}}(t_i, t_j)]_{\{1 \leq i, j \leq q\}} \in \mathbb{R}^{q \times q}$ is positive semi-definite.

2.2 Covariance Estimation by Bivariate Penalized Splines

Suppose that the observed data take the form $\{(\mathbf{y}_{ij}, t_{ij}) : i = 1, \dots, n; j = 1, \dots, m_i\}$, where $t_{ij} \in \mathcal{T}$ is the observed time point, $\mathbf{y}_{ij} = \left(y_{ij}^{(1)}, \dots, y_{ij}^{(p)}\right)^\top \in \mathbb{R}^p$ is the observed multivariate response, n is the number of subjects, and m_i is the number of observations for subject i . The model is

$$\mathbf{y}_{ij} = \mathbf{x}_i(t_{ij}) + \boldsymbol{\epsilon}_{ij} = \boldsymbol{\mu}(t_{ij}) + \sum_{\ell=1}^{\infty} \xi_{i\ell} \boldsymbol{\Psi}_\ell(t_{ij}) + \boldsymbol{\epsilon}_{ij}, \quad (3)$$

where $\mathbf{x}_i(t_{ij}) = \left(x_i^{(1)}(t_{ij}), \dots, x_i^{(p)}(t_{ij})\right)^\top$ is a realization of the stochastic process \mathbf{x}_i in \mathcal{H} , $\boldsymbol{\epsilon}_{ij} = \left(\epsilon_{ij}^{(1)}, \dots, \epsilon_{ij}^{(p)}\right)^\top$, and $\epsilon_{ij}^{(k)}$ are random noises with zero means and variances σ_k^2 and are independent across i, j and k .

The interest is in estimating the covariance functions $C_{kk'}$. We adopt a three-step procedure. In the first step, empirical estimates of the covariance functions are constructed. Let $r_{ij}^{(k)} = y_{ij}^{(k)} - \mu^{(k)}(t_{ij})$ be the residuals and $C_{ij_1 j_2}^{(kk')} = r_{ij_1}^{(k)} r_{ij_2}^{(k')}$ be the auxiliary variables. Note that $\mathbb{E}\left(C_{ij_1 j_2}^{(kk')}\right) = C_{kk'}(t_{ij_1}, t_{ij_2}) + \sigma_k^2 \mathbf{1}_{\{k=k', j_1=j_2\}}$ for $1 \leq j_1, j_2 \leq m_i$. Thus, $C_{ij_1 j_2}^{(kk')}$ is an unbiased estimate of $C_{kk'}(t_{ij_1}, t_{ij_2})$ whenever $k \neq k'$ or $j_1 \neq j_2$. In the second step, the noisy auxiliary variables are smoothed to obtain smooth estimates of the covariance functions. For smoothing, we use bivariate P -splines (Eilers and Marx, 2003) because it is an automatic smoother and is computationally simple. In the final step, we pool all estimates of the individual covariance functions and use an extra step of eigen-decomposition to obtain refined estimates of covariance functions. The refined estimates lead to a covariance operator that is properly defined, i.e., positive semi-definite. In practice, the mean functions μ_{ks} are unknown and we estimate them using P -splines (Eilers and Marx, 1996) with the smoothing parameters selected by leave-one-subject-out cross validation; see Appendix A for details. Denote the estimates by $\hat{\mu}^{(k)}$. Let $\hat{r}_{ij}^{(k)} = y_{ij}^{(k)} - \hat{\mu}^{(k)}(t_{ij})$ and $\hat{C}_{ij_1 j_2}^{(kk')} = \hat{r}_{ij_1}^{(k)} \hat{r}_{ij_2}^{(k')}$, the actual auxiliary variables.

The bivariate P -splines model $C_{kk'}(s, t)$ uses tensor-product splines $G_{kk'}(s, t)$ for $1 \leq k, k' \leq p$. Specifically, $G_{kk'}(s, t) = \sum_{1 \leq \gamma_1, \gamma_2 \leq c} \theta_{\gamma_1 \gamma_2}^{(kk')} B_{\gamma_1}(s) B_{\gamma_2}(t)$, where $\boldsymbol{\Theta}_{kk'} = \left[\theta_{\gamma_1 \gamma_2}^{(kk')}\right]_{1 \leq \gamma_1, \gamma_2 \leq c} \in \mathbb{R}^{c \times c}$ is a coefficient matrix, $\{B_1(\cdot), \dots, B_c(\cdot)\}$ is the collection of B-spline basis functions in the unit interval, and c is the number of equally-spaced

interior knots plus the order (degree plus 1) of the B-splines. Because $C_{kk'}(s, t) = C_{k'k}(t, s) = \text{Cov}\{x^{(k)}(s), x^{(k')}(t)\}$, it is reasonable to impose the assumption that

$$\boldsymbol{\Theta}_{kk'} = \boldsymbol{\Theta}_{k'k}^\top$$

so that $G_{kk'}(s, t) = G_{k'k}(t, s)$. Therefore, in the rest of the section, we consider only $k \leq k'$.

Let $\mathbf{D} \in \mathbb{R}^{(c-2) \times c}$ denote a second-order differencing matrix such that for a vector $\mathbf{a} = (a_1, \dots, a_c)^\top \in \mathbb{R}^c$, $\mathbf{D}\mathbf{a} = (a_3 - 2a_2 + a_1, a_4 - 2a_3 + a_2, \dots, a_c - 2a_{c-1} + a_{c-2})^\top \in \mathbb{R}^{c-2}$. Also let $\|\cdot\|_F$ denote the Frobenius norm. For the cross-covariance function $C_{kk'}(s, t)$ with $k < k'$, the bivariate P -splines estimate the coefficient matrix $\boldsymbol{\Theta}_{kk'}$ by $\hat{\boldsymbol{\Theta}}_{kk'}$ which minimizes the penalized least squares

$$\sum_{i=1}^n \sum_{1 \leq j_1, j_2 \leq m_i} \left\{ G_{kk'}(t_{ij_1}, t_{ij_2}) - \hat{C}_{ij_1 j_2}^{(kk')} \right\}^2 + \lambda_{kk'1} \|\mathbf{D}\boldsymbol{\Theta}_{kk'}\|_F^2 + \lambda_{kk'2} \|\mathbf{D}\boldsymbol{\Theta}_{kk'}^\top\|_F^2, \quad (4)$$

where $\lambda_{kk'1}$ and $\lambda_{kk'2}$ are two nonnegative smoothing parameters that balance the model fit and smoothness of the estimate and will be determined later. Indeed, the column penalty $\|\mathbf{D}\boldsymbol{\Theta}_{kk'}\|_F^2$ penalizes the 2nd order consecutive differences of the columns of $\boldsymbol{\Theta}_{kk'}$ and similarly, the row penalty $\|\mathbf{D}\boldsymbol{\Theta}_{kk'}^\top\|_F^2$ penalizes the 2nd order consecutive differences of the rows of $\boldsymbol{\Theta}_{kk'}$. The two penalty terms are essentially penalizing the 2nd order partial derivatives of $G_{kk'}(s, t)$ along the s and t directions, respectively. The two smoothing parameters are allowed to differ to accommodate different levels of smoothing along the two directions.

For the auto-covariance functions $C_{kk}(s, t)$ with $k = 1, \dots, p$, we conduct bivariate covariance smoothing by enforcing the following constraint on the coefficient matrix $\boldsymbol{\Theta}_{kk}$ (Xiao et al., 2018),

$$\boldsymbol{\Theta}_{kk} = \boldsymbol{\Theta}_{kk}^\top. \quad (5)$$

It follows that $G_{kk}(s, t)$ is a symmetric function. Then the coefficient matrix $\boldsymbol{\Theta}_{kk}$ and the error variance σ_k^2 are jointly estimated by $\hat{\boldsymbol{\Theta}}_{kk}$ and $\hat{\sigma}_k^2$, which minimize the penalized least squares

$$\sum_{i=1}^n \sum_{1 \leq j_1 \leq j_2 \leq m_i} \left\{ G_{kk}(t_{ij_1}, t_{ij_2}) + \sigma_k^2 1_{\{j_1=j_2\}} - \hat{C}_{ij_1 j_2}^{(kk)} \right\}^2 + \lambda_k \|\mathbf{D}\boldsymbol{\Theta}_{kk}\|_F^2, \quad (6)$$

over all symmetric Θ_{kk} and λ_k is a smoothing parameter. Note that the two penalty terms in (4) become the same when Θ_{kk} is symmetric and thus only one smoothing parameter is needed for auto-covariance estimation.

2.2.1 Estimation

We first introduce the notation. Let $\text{vec}(\cdot)$ be an operator that stacks the columns of a matrix into a column vector and denote by \otimes the Kronecker product. Fix k and k' with $k \leq k'$. Let $\theta_{kk'} = \text{vec}(\Theta_{kk'}) \in \mathbb{R}^{c^2}$ be a vector of the coefficients and $\mathbf{b}(t) = \{B_1(t), \dots, B_c(t)\}^\top \in \mathbb{R}^c$ denotes the B-spline base. Then

$$G_{kk'}(s, t) = \mathbf{b}(s)^\top \Theta_{kk'} \mathbf{b}(t) = \{\mathbf{b}(t) \otimes \mathbf{b}(s)\}^\top \theta_{kk'}.$$

We now organize the auxiliary responses $\hat{C}_{ij_1 j_2}^{(kk')}$ for each pair of k and k' . Let $\hat{\mathbf{C}}_{ij}^{(kk')} = (\hat{C}_{ij1}^{(kk')}, \dots, \hat{C}_{ijm_i}^{(kk')})^\top \in \mathbb{R}^{m_i}$, $\hat{\mathbf{C}}_i^{(kk')} = (\hat{\mathbf{C}}_{i1}^{(kk')\top}, \dots, \hat{\mathbf{C}}_{im_i}^{(kk')\top})^\top \in \mathbb{R}^{m_i^2}$, and finally $\hat{\mathbf{C}}^{(kk')} = (\hat{\mathbf{C}}_1^{(kk')\top}, \dots, \hat{\mathbf{C}}_n^{(kk')\top})^\top \in \mathbb{R}^N$, where $N = \sum_{i=1}^n m_i^2$ is the total number of auxiliary responses for each pair of k and k' . As for the B-splines, let $\mathbf{B}_{ij} = [\mathbf{b}(t_{i1}), \dots, \mathbf{b}(t_{im_i})] \otimes \mathbf{b}(t_{ij}) \in \mathbb{R}^{c^2 \times m_i}$, $\mathbf{B}_i = [\mathbf{B}_{i1}, \dots, \mathbf{B}_{im_i}]^\top \in \mathbb{R}^{m_i^2 \times c^2}$ and $\mathbf{B} = [\mathbf{B}_1^\top, \dots, \mathbf{B}_n^\top]^\top \in \mathbb{R}^{N \times c^2}$. Note that the above B-spline design matrices are the same for every pair of k and k' , thus dramatically reducing the computations.

For estimation of the cross-covariance functions $C_{kk'}$ with $k < k'$, the penalized least squares in (4) can be rewritten as

$$\left(\hat{\mathbf{C}}^{(kk')} - \mathbf{B}\theta_{kk'}\right)^\top \left(\hat{\mathbf{C}}^{(kk')} - \mathbf{B}\theta_{kk'}\right) + \lambda_{kk'1} \theta_{kk'}^\top \mathbf{P}_1 \theta_{kk'} + \lambda_{kk'2} \theta_{kk'}^\top \mathbf{P}_2 \theta_{kk'}, \quad (7)$$

where $\mathbf{P}_1 = \mathbf{I}_c \otimes \mathbf{D}^\top \mathbf{D}$ and $\mathbf{P}_2 = \mathbf{D}^\top \mathbf{D} \otimes \mathbf{I}_c$. The expression in (7) is a quadratic function of the coefficient vector $\theta_{kk'}$. Therefore, we derive that

$$\hat{\theta}_{kk'} = \left(\mathbf{B}^\top \mathbf{B} + \lambda_{kk'1} \mathbf{P}_1 + \lambda_{kk'2} \mathbf{P}_2\right)^{-1} \mathbf{B}^\top \hat{\mathbf{C}}^{(kk')}$$

and the estimate of the cross-covariance function $C_{kk'}(s, t)$ is $\hat{C}_{kk'}(s, t) = \{\mathbf{b}(t) \otimes \mathbf{b}(s)\}^\top \hat{\theta}_{kk'}$.

For estimation of the auto-covariance functions, because of the constraint on the coefficient matrix in (5), let $\eta_k \in \mathbb{R}^{c(c+1)/2}$ be a vector obtained by stacking the

columns of the lower triangle of Θ_{kk} and let $\mathbf{G}_c \in \mathbb{R}^{c^2 \times c(c+1)/2}$ be a duplication matrix such that $\theta_{kk} = \mathbf{G}_c \eta_k$ (Page 246, Seber 2007). Let $\mathbf{Z}_i = \text{vec}(\mathbf{I}_{m_i}) \in \mathbb{R}^{m_i^2}$ and $\mathbf{Z} = (\mathbf{Z}_1^\top, \dots, \mathbf{Z}_n^\top)^\top \in \mathbb{R}^N$. Finally let $\beta_k = (\eta_k^\top, \sigma_k^2)^\top \in \mathbb{R}^{\tilde{c}}$ with $\tilde{c} = c(c+1)/2 + 1$. It follows that the penalized least squares in (6) can be rewritten as

$$\left(\widehat{\mathbf{C}}^{(kk)} - \mathbf{X}\beta_k\right)^\top \left(\widehat{\mathbf{C}}^{(kk)} - \mathbf{X}\beta_k\right) + \lambda_k \beta_k^\top \mathbf{Q} \beta_k,$$

where $\mathbf{X} = [\mathbf{B}, \mathbf{Z}] \in \mathbb{R}^{N \times \tilde{c}}$ and $\mathbf{Q} = \text{blockdiag}\{\mathbf{G}_c^\top (\mathbf{I}_c \otimes \mathbf{D}\mathbf{D}^\top) \mathbf{G}_c^\top, 0\} \in \mathbb{R}^{\tilde{c} \times \tilde{c}}$. Therefore, we obtain

$$\widehat{\beta}_k = (\widehat{\eta}_k^\top, \widehat{\sigma}_k^2)^\top = (\mathbf{X}^\top \mathbf{X} + \lambda_k \mathbf{Q})^{-1} \mathbf{X}^\top \widehat{\mathbf{C}}^{(kk)}.$$

It follows that $\widehat{\theta}_{kk} = \mathbf{G}_c \widehat{\eta}_k$ and the estimate of the auto-covariance function $C_{kk}(s, t)$ is $\widehat{C}_{kk}(s, t) = \{\mathbf{b}(t) \otimes \mathbf{b}(s)\}^\top \widehat{\theta}_{kk}$.

The above estimates of covariance functions may not lead to a positive semi-definite covariance operator and thus have to be refined. We pool all estimates together and we shall use the following proposition.

Proposition 1. *Assume that $C_{kk'}(s, t) = \mathbf{b}(s)^\top \Theta_{kk'} \mathbf{b}(t)$. Let $\mathbf{G} = \int \mathbf{b}(t) \mathbf{b}(t)^\top dt \in \mathbb{R}^{c \times c}$ and assume that \mathbf{G} is positive definite (Zhou et al., 1998). Then $\left[\mathbf{G}^{\frac{1}{2}} \Theta_{kk'} \mathbf{G}^{\frac{1}{2}}\right]_{1 \leq k, k' \leq p} \in \mathbb{R}^{pc \times pc}$ admits the spectral decomposition, $\sum_{\ell=1}^{\infty} d_\ell \mathbf{u}_\ell \mathbf{u}_\ell^\top$, where d_ℓ is the ℓ th largest eigenvalue of the covariance operator $\mathbf{\Gamma}$, and $\mathbf{u}_\ell = \left\{\mathbf{u}_\ell^{(1), \top}, \dots, \mathbf{u}_\ell^{(p), \top}\right\}^\top \in \mathbb{R}^{pc}$ is the associated eigenvector with $\mathbf{u}_\ell^{(k)} \in \mathbb{R}^c$ and such that $\Psi_\ell^{(k)}(t) = \mathbf{b}(t)^\top \mathbf{G}^{-\frac{1}{2}} \mathbf{u}_\ell^{(k)}$.*

The proof is provided in Appendix B. Proposition 1 implies that, with the tensor-product B-spline representation of the covariance functions, one spectral decomposition gives us the eigenvalues and eigenfunctions. In particular, the eigenfunctions $\Psi_\ell^{(k)}(t)$ are linear combinations of the B-spline basis functions, which means that they can be straightforwardly evaluated, an advantage of spline-based methods compared to other smoothing methods for which eigenfunctions are approximated by spectral decompositions of the covariance functions evaluated at a grid of time points.

Once we have $\widehat{\Theta}_{kk'}$, the estimate of the coefficient matrix $\Theta_{kk'}$, the spectral decomposition of $[\mathbf{G}^{\frac{1}{2}} \widehat{\Theta}_{kk'} \mathbf{G}^{\frac{1}{2}}]_{kk'}$ gives us estimates \widehat{d}_ℓ and $\widehat{\mathbf{u}}_\ell = \left\{\widehat{\mathbf{u}}_\ell^{(1), \top}, \dots, \widehat{\mathbf{u}}_\ell^{(p), \top}\right\}^\top$. We discard negative \widehat{d}_ℓ to ensure that the multivariate covariance operator is positive semi-definite and this leads to a refined estimate of the coefficient matrix $\Theta_{kk'}$,

$\tilde{\Theta}_{kk'} = \mathbf{G}^{-\frac{1}{2}} \left\{ \sum_{\ell: \hat{d}_\ell > 0} \hat{d}_\ell \hat{\mathbf{u}}_\ell^{(k)} \hat{\mathbf{u}}_\ell^{(k')\top} \right\} \mathbf{G}^{-\frac{1}{2}}$. Then the refined estimate of the covariance functions is $\tilde{C}_{kk'}(s, t) = \mathbf{b}(s)^\top \tilde{\Theta}_{kk'} \mathbf{b}(t)$. Proposition 1 also suggests that the eigenfunctions can be estimated by $\tilde{\Psi}_\ell^{(k)}(t) = \mathbf{b}(t)^\top \mathbf{G}^{-\frac{1}{2}} \hat{\mathbf{u}}_\ell^{(k)}$.

For principal component analysis or curve prediction in practice, one may select further the number of principal components by either the proportion of variance explained (PVE) (Greven et al., 2010) or an AIC-type criterion (Li et al., 2013). Here, we follow Greven et al. (2010) using PVE with a value of 0.99.

2.2.2 Selection of Smoothing Parameters

We select the smoothing parameters in each auto-covariance/cross-covariance estimation using leave-one-subject-out cross-validation; see, e.g., Yao et al. (2005) and Xiao et al. (2018). A fast approximate algorithm for the auto-covariance has been derived in Xiao et al. (2018). So we focus on the cross-covariance and use the notation in (7). Note that there are two smoothing parameters for each cross-covariance estimation.

For simplicity, we suppress the superscript and subscript kk' in (7). Let $\tilde{\mathbf{C}}_i^{[i]}$ be the prediction of the auxiliary responses $\hat{\mathbf{C}}_i$ from the estimate using data without the i th subject. Let $\|\cdot\|$ be the Euclidean norm and the cross-validation error is

$$\text{iCV} = \sum_{i=1}^n \left\| \hat{\mathbf{C}}_i - \tilde{\mathbf{C}}_i^{[i]} \right\|^2. \quad (8)$$

Let $\mathbf{S} = \mathbf{B}(\mathbf{B}^\top \mathbf{B} + \lambda_1 \mathbf{P}_1 + \lambda_2 \mathbf{P}_2)^{-1} \mathbf{B}^\top \in \mathbb{R}^{N \times N}$, $\mathbf{S}_i = \mathbf{B}_i(\mathbf{B}^\top \mathbf{B} + \lambda_1 \mathbf{P}_1 + \lambda_2 \mathbf{P}_2)^{-1} \mathbf{B}^\top \in \mathbb{R}^{m_i^2 \times N}$, and $\mathbf{S}_{ii} = \mathbf{B}_i(\mathbf{B}^\top \mathbf{B} + \lambda_1 \mathbf{P}_1 + \lambda_2 \mathbf{P}_2)^{-1} \mathbf{B}_i^\top \in \mathbb{R}^{m_i^2 \times m_i^2}$. Then a short-cut formula for (8) is

$$\text{iCV} = \sum_{i=1}^n \left\| \left(\mathbf{I}_{m_i^2} - \mathbf{S}_{ii} \right)^{-1} \left(\mathbf{S}_i \hat{\mathbf{C}} - \hat{\mathbf{C}}_i \right) \right\|^2.$$

Similar to Xu and Huang (2012) and Xiao et al. (2018), the iCV can be further simplified by adopting the approximation $(\mathbf{I}_{m_i^2} - \mathbf{S}_{ii})^{-2} = \mathbf{I}_{m_i^2} + 2\mathbf{S}_{ii}$, which results in the generalized cross validation, denoted by iGCV,

$$\text{iGCV} = \left\| \hat{\mathbf{C}} - \mathbf{S} \hat{\mathbf{C}} \right\|^2 + 2 \sum_{i=1}^n \left(\mathbf{S}_i \hat{\mathbf{C}} - \hat{\mathbf{C}}_i \right)^\top \mathbf{S}_{ii} \left(\mathbf{S}_i \hat{\mathbf{C}} - \hat{\mathbf{C}}_i \right). \quad (9)$$

While iGCV is much easier to compute than iCV, the formula in (9) is still computationally expensive to compute. Indeed, the smoother matrix \mathbf{S} is of dimension

2500 \times 2500 if $n = 100$ and $m_i = m = 5$ for all i . Thus, we further simplify the formula.

Let $\mathbf{G}_n = \mathbf{B}^\top \mathbf{B}$, $\tilde{\mathbf{B}} = \mathbf{B} \mathbf{G}_n^{-1/2} \in \mathbb{R}^{N \times c^2}$, $\tilde{\mathbf{B}}_i = \mathbf{B}_i \mathbf{G}_n^{-1/2} \in \mathbb{R}^{m_i^2 \times c^2}$, $\mathbf{f} = \tilde{\mathbf{B}}^\top \hat{\mathbf{C}} \in \mathbb{R}^{c^2}$, $\mathbf{f}_i = \tilde{\mathbf{B}}_i^\top \hat{\mathbf{C}}_i \in \mathbb{R}^{c^2}$, and $\mathbf{L}_i = \tilde{\mathbf{B}}_i^\top \tilde{\mathbf{B}}_i \in \mathbb{R}^{c^2 \times c^2}$. Also let $\tilde{\mathbf{P}}_1 = \mathbf{G}_n^{-1/2} \mathbf{P}_1 \mathbf{G}_n^{-1/2} \in \mathbb{R}^{c^2 \times c^2}$, $\tilde{\mathbf{P}}_2 = \mathbf{G}_n^{-1/2} \mathbf{P}_2 \mathbf{G}_n^{-1/2} \in \mathbb{R}^{c^2 \times c^2}$, and $\Sigma = \mathbf{I}_{c^2} + \lambda_1 \tilde{\mathbf{P}}_1 + \lambda_2 \tilde{\mathbf{P}}_2$. Then (9) can be simplified as

$$\text{iGCV} = \left\| \hat{\mathbf{C}} \right\|^2 - 2\mathbf{f}^\top \Sigma^{-1} \mathbf{f} + \mathbf{f}^\top \Sigma^{-2} \mathbf{f} + 2 \sum_{i=1}^n (\mathbf{L}_i \Sigma^{-1} \mathbf{f} - \mathbf{f}_i)^\top \Sigma^{-1} (\mathbf{L}_i \Sigma^{-1} \mathbf{f} - \mathbf{f}_i). \quad (10)$$

Note that Σ has two smoothing parameters. Following Wood (2000), we use an equivalent parameterization $\Sigma = \mathbf{I} + \rho \{w \tilde{\mathbf{P}}_1 + (1-w) \tilde{\mathbf{P}}_2\}$, where $\rho = \lambda_1 + \lambda_2$ represents the overall smoothing level and $w = \lambda_1 \rho^{-1} \in [0, 1]$ is the relative weight of λ_1 . We conduct a two-dimensional grid search of (ρ, w) as follows. For a given w , let $\mathbf{U} \text{diag}(\mathbf{s}) \mathbf{U}^\top$ be the eigendecomposition of $w \tilde{\mathbf{P}}_1 + (1-w) \tilde{\mathbf{P}}_2$, where $\mathbf{U} \in \mathbb{R}^{c^2 \times c^2}$ is an orthonormal matrix and $\mathbf{s} = (s_1, \dots, s_{c^2}) \in \mathbb{R}^{c^2}$ is the vector of eigenvalues. Then $\Sigma^{-1} = \mathbf{U} \text{diag}(\tilde{\mathbf{d}}) \mathbf{U}^\top$ with $\tilde{\mathbf{d}} = 1/(1 + \rho \mathbf{s}) \in \mathbb{R}^{c^2}$.

Proposition 2. *Let \odot stand for the point-wise multiplication. Then,*

$$\text{iGCV} = \left\| \hat{\mathbf{C}} \right\|^2 + (\tilde{\mathbf{f}} \odot \tilde{\mathbf{d}})^\top (\tilde{\mathbf{f}} \odot \tilde{\mathbf{d}}) - 2\tilde{\mathbf{d}}^\top \mathbf{g} - 4\tilde{\mathbf{d}}^\top \mathbf{F} \tilde{\mathbf{d}} + 2\tilde{\mathbf{d}}^\top \left[\sum_{i=1}^n \left\{ \tilde{\mathbf{L}}_i (\tilde{\mathbf{f}} \odot \tilde{\mathbf{d}}) \right\} \odot \left\{ \tilde{\mathbf{L}}_i (\tilde{\mathbf{f}} \odot \tilde{\mathbf{d}}) \right\} \right],$$

where $\tilde{\mathbf{f}}_i = \mathbf{U}^\top \mathbf{f}_i \in \mathbb{R}^{c^2}$, $\tilde{\mathbf{f}} = \mathbf{U}^\top \mathbf{f} \in \mathbb{R}^{c^2}$, $\mathbf{g} = \tilde{\mathbf{f}} \odot \tilde{\mathbf{f}} - \sum_{i=1}^n \tilde{\mathbf{f}}_i \odot \tilde{\mathbf{f}}_i \in \mathbb{R}^{c^2}$, $\tilde{\mathbf{L}}_i = \mathbf{U}^\top \mathbf{L}_i \mathbf{U} \in \mathbb{R}^{c^2 \times c^2}$, and $\mathbf{F} = \sum_{i=1}^n (\tilde{\mathbf{f}}_i \tilde{\mathbf{f}}_i^\top) \odot \tilde{\mathbf{L}}_i \in \mathbb{R}^{c^2 \times c^2}$.

The proof is provided in Appendix B. For each w , note that only $\tilde{\mathbf{d}}$ depends on ρ and needs to be calculated repeatedly, and all other terms need to be calculated only once. The entire algorithm is presented in Algorithm 1. We give an evaluation of the complexity of the proposed algorithm. Assume that $m_i = m$ for all i . The first initialization (step 1) requires $O(nm^2c^2 + nc^4 + c^6)$ computations. For each w , the second initialization (step 3) also requires $O\{nc^4 \min(m^2, c^2) + c^6\}$ computations. For each ρ , steps 5-10 requires $O(nc^4)$ computations. Therefore, the formula in Proposition 2 is most efficient to calculate for sparse data with small numbers of observations per subject, i.e., m_i s are small.

<div style="margin-bottom: 10px;"> Input: $\mathbf{B}, \hat{\mathbf{C}}, \mathbf{P}_1, \mathbf{P}_2, \boldsymbol{\rho} = \{\rho_1, \dots, \rho_K\}^\top, \mathbf{w} = \{w_1, \dots, w_K\}^\top$ </div> <div style="margin-bottom: 10px;"> Output: $\{\rho^*, w^*\}$ </div> <div> 1 Initialize $\ \hat{\mathbf{C}}\ ^2, \tilde{\mathbf{P}}_1, \tilde{\mathbf{P}}_2, \mathbf{G}_n^{-1/2}, \tilde{\mathbf{B}}, \tilde{\mathbf{B}}_i, \mathbf{f}, \mathbf{f}_i, \mathbf{L}_i$ for $i = 1, \dots, n$; 2 foreach w <i>in</i> \mathbf{w} do 3 Initialize $\mathbf{s}, \tilde{\mathbf{f}}, \tilde{\mathbf{f}}_i, \mathbf{g}, \mathbf{F}, \tilde{\mathbf{L}}_i, i = 1, \dots, n$; 4 foreach ρ <i>in</i> $\boldsymbol{\rho}$ do 5 $\tilde{\mathbf{d}} \leftarrow 1/(1 + \rho\mathbf{s})$; 6 $I \leftarrow (\tilde{\mathbf{f}} \odot \tilde{\mathbf{d}})^\top (\tilde{\mathbf{f}} \odot \tilde{\mathbf{d}})$; 7 $II \leftarrow -2\tilde{\mathbf{d}}^\top \mathbf{g}$; 8 $III \leftarrow -4\tilde{\mathbf{d}}^\top \mathbf{F}\tilde{\mathbf{d}}$; 9 $IV \leftarrow 2\tilde{\mathbf{d}}^\top \left[\sum_{i=1}^n \left\{ \tilde{\mathbf{L}}_i(\tilde{\mathbf{f}} \odot \tilde{\mathbf{d}}) \right\} \odot \left\{ \tilde{\mathbf{L}}_i(\tilde{\mathbf{f}} \odot \tilde{\mathbf{d}}) \right\} \right]$; 10 $\text{iGCV} \leftarrow \ \hat{\mathbf{C}}\ ^2 + I + II + III + IV$; 11 end 12 end 13 $\{\rho^*, w^*\} \leftarrow \arg \min_{\rho, w} \text{iGCV}$; </div>

Algorithm 1: Selection of smoothing parameters

2.3 Prediction

For prediction, assume that the smooth curve $\mathbf{x}_i(t)$ is generated from a multivariate Gaussian process. Suppose that we want to predict the i th multivariate response $\mathbf{x}_i(t)$ at $\{s_{i1}, \dots, s_{im}\}$ for $m \geq 1$. Let $\mathbf{y}_i = (y_{i1}^{(1)}, \dots, y_{im_i}^{(1)}, \dots, y_{i1}^{(p)}, \dots, y_{im_i}^{(p)})^\top$ be the observations at $\{t_{i1}, \dots, t_{im_i}\}$. Also let $\boldsymbol{\mu}_i^o = (\mu^{(1)}(t_{i1}), \dots, \mu^{(1)}(t_{im_i}), \dots, \mu^{(p)}(t_{i1}), \dots, \mu^{(p)}(t_{im_i}))^\top$ be the vector of mean functions at the observed time points and $\boldsymbol{\mu}_i^n = (\mu^{(1)}(s_{i1}), \dots, \mu^{(1)}(s_{im}), \dots, \mu^{(p)}(s_{i1}), \dots, \mu^{(p)}(s_{im}))^\top$ be the vector of mean functions at the time points for prediction. It follows that

$$\begin{pmatrix} \mathbf{y}_i \\ \mathbf{x}_i \end{pmatrix} \sim \mathcal{N} \left\{ \begin{pmatrix} \boldsymbol{\mu}_i^o \\ \boldsymbol{\mu}_i^n \end{pmatrix}, \begin{pmatrix} \text{Cov}(\mathbf{y}_i) & \text{Cov}(\mathbf{y}_i, \mathbf{x}_i) \\ \text{Cov}(\mathbf{x}_i, \mathbf{y}_i) & \text{Cov}(\mathbf{x}_i) \end{pmatrix} \right\}.$$

Thus, we obtain

$$\mathbb{E}(\mathbf{x}_i | \mathbf{y}_i) = \text{Cov}(\mathbf{x}_i, \mathbf{y}_i) \text{Cov}(\mathbf{y}_i)^{-1} (\mathbf{y}_i - \boldsymbol{\mu}_i^o) + \boldsymbol{\mu}_i^n,$$

$$\text{Cov}(\mathbf{x}_i | \mathbf{y}_i) = \text{Cov}(\mathbf{x}_i) - \text{Cov}(\mathbf{x}_i, \mathbf{y}_i) \text{Cov}(\mathbf{y}_i)^{-1} \text{Cov}(\mathbf{y}_i, \mathbf{x}_i),$$

Let $\mathbf{b}_i^o = [\mathbf{b}(t_{i1}), \dots, \mathbf{b}(t_{im_i})]^\top$, $\mathbf{b}_i^n = [\mathbf{b}(s_{i1}), \dots, \mathbf{b}(s_{im})]^\top$, $\mathbf{B}_i^o = \mathbf{I}_p \otimes \mathbf{b}_i^o$, $\mathbf{B}_i^n = \mathbf{I}_p \otimes \mathbf{b}_i^n$. Also let $\tilde{\boldsymbol{\Theta}} = [\tilde{\boldsymbol{\Theta}}_{kk'}]_{1 \leq k, k' \leq p} \in \mathbb{R}^{pc \times pc}$. Then $\text{Cov}(\mathbf{y}_i)$ is approximated by $\mathbf{B}_i^o \tilde{\boldsymbol{\Theta}} \mathbf{B}_i^{o, \top} + \text{diag}(\sigma_1^2, \dots, \sigma_p^2) \otimes \mathbf{I}_{m_i}$, and $\text{Cov}(\mathbf{x}_i)$ and $\text{Cov}(\mathbf{y}_i, \mathbf{x}_i)$ are approximated by $\mathbf{B}_i^n \tilde{\boldsymbol{\Theta}} \mathbf{B}_i^{n, \top}$ and $\mathbf{B}_i^o \tilde{\boldsymbol{\Theta}} \mathbf{B}_i^{n, \top}$, respectively.

Plugging in the estimates, we predict \mathbf{x}_i by

$$\begin{aligned} \hat{\mathbf{x}}_i &= \left(\hat{x}_i^{(1)}(s_{i1}), \dots, \hat{x}_i^{(1)}(s_{im}), \dots, \hat{x}_i^{(p)}(s_{i1}), \dots, \hat{x}_i^{(p)}(s_{im}) \right)^\top \\ &= \left(\mathbf{B}_i^n \tilde{\boldsymbol{\Theta}} \mathbf{B}_i^{o, \top} \right) \hat{\mathbf{V}}_i^{-1} (\mathbf{y}_i - \hat{\boldsymbol{\mu}}_i^o) + \hat{\boldsymbol{\mu}}_i^n, \end{aligned}$$

where $\hat{\boldsymbol{\mu}}_i^o = (\hat{\mu}^{(1)}(t_{i1}), \dots, \hat{\mu}^{(1)}(t_{im_i}), \dots, \hat{\mu}^{(p)}(t_{i1}), \dots, \hat{\mu}^{(p)}(t_{im_i}))^\top$ is the estimate of $\boldsymbol{\mu}_i^o$, $\hat{\boldsymbol{\mu}}_i^n = (\hat{\mu}^{(1)}(s_{i1}), \dots, \hat{\mu}^{(1)}(s_{im}), \dots, \hat{\mu}^{(p)}(s_{i1}), \dots, \hat{\mu}^{(p)}(s_{im}))^\top$ is the estimate of $\boldsymbol{\mu}_i^n$, $\hat{\mathbf{V}}_i = \mathbf{B}_i^o \tilde{\boldsymbol{\Theta}} \mathbf{B}_i^{o, \top} + \text{diag}(\hat{\sigma}_1^2, \dots, \hat{\sigma}_p^2) \otimes \mathbf{I}_{m_i}$. An approximate covariance matrix for $\hat{\mathbf{x}}_i$ is

$$\widehat{\text{Cov}}(\mathbf{x}_i | \mathbf{y}_i) = \mathbf{B}_i^n \tilde{\boldsymbol{\Theta}} \mathbf{B}_i^{n, \top} - \left(\mathbf{B}_i^n \tilde{\boldsymbol{\Theta}} \mathbf{B}_i^{o, \top} \right) \hat{\mathbf{V}}_i^{-1} \left(\mathbf{B}_i^o \tilde{\boldsymbol{\Theta}} \mathbf{B}_i^{o, \top} \right)^\top.$$

Therefore, a 95% point-wise confidence interval for the k th response is given by

$$\hat{x}_i^{(k)}(s_{ij}) \pm 1.96 \sqrt{\widehat{\text{Var}} \left(x_i^{(k)}(s_{ij}) | \mathbf{y}_i \right)},$$

where $\widehat{\text{Var}}\left(x_i^{(k)}(s_{ij})|\mathbf{y}_i\right)$ can be extracted from the diagonal of $\widehat{\text{Cov}}(\mathbf{x}_i|\mathbf{y}_i)$.

Finally, we predict the first $L \geq 1$ scores $\boldsymbol{\xi}_i = (\xi_{i1}, \dots, \xi_{iL})^\top$ for the i th subject. Note that $\xi_{i\ell} = \int \boldsymbol{\Psi}_\ell(t)^\top \{\mathbf{x}_i(t) - \boldsymbol{\mu}(t)\} dt$. With a similar derivation as above, $\mathbf{x}_i(t) - \boldsymbol{\mu}(t)$ can be predicted by $\{\mathbf{I}_p \otimes \mathbf{b}(t)\}^\top \tilde{\boldsymbol{\Theta}} \mathbf{B}_i^{o,\top} \hat{\mathbf{V}}_i^{-1}(\mathbf{y}_i - \hat{\boldsymbol{\mu}}_i^o)$. By Proposition 1, the eigenfunctions $\boldsymbol{\Psi}_\ell^{(k)}(t)$ are estimated by $\mathbf{b}(t)^\top \mathbf{G}^{-\frac{1}{2}} \hat{\mathbf{u}}_\ell^{(k)}$ and thus $\boldsymbol{\Psi}_\ell(t)^\top = \hat{\mathbf{u}}_\ell^\top \{\mathbf{I}_p \otimes \mathbf{G}^{-\frac{1}{2}} \mathbf{b}(t)\}$. It follows that

$$\hat{\xi}_{i\ell} = \hat{\mathbf{u}}_\ell^\top \left(\mathbf{I}_p \otimes \mathbf{G}^{\frac{1}{2}} \right) \tilde{\boldsymbol{\Theta}} \mathbf{B}_i^{o,\top} \hat{\mathbf{V}}_i^{-1}(\mathbf{y}_i - \hat{\boldsymbol{\mu}}_i^o).$$

3 Simulations

We evaluate the finite sample performance of the proposed method (denoted by mFACES) against mFPCA via a synthetic simulation study and a simulation study mimicking the ADNI data in the real data example. Here, we report the details and results of the former as the conclusions remain the same for the latter and is provided in the supplement.

3.1 Simulation Settings and Evaluation Criterias

We generate data by model (3) with $p = 3$ responses. The mean functions are $\boldsymbol{\mu}(t) = [5 \sin(2\pi t), 5 \cos(2\pi t), 5(t-1)^2]^\top$. We first specify the auto-covariance functions. Let $\boldsymbol{\Phi}_1(t) = [\sqrt{2} \sin(2\pi t), \sqrt{2} \cos(4\pi t), \sqrt{2} \sin(4\pi t)]$, $\boldsymbol{\Phi}_2(t) = [\sqrt{2} \cos(\pi t), \sqrt{2} \cos(2\pi t), \sqrt{2} \cos(3\pi t)]$, and $\boldsymbol{\Phi}_3(t) = [\sqrt{2} \sin(\pi t), \sqrt{2} \sin(2\pi t), \sqrt{2} \sin(3\pi t)]$. Also let

$$\boldsymbol{\Lambda}_{11} = \begin{pmatrix} 3 & 0 & 0 \\ 0 & 1.5 & 0 \\ 0 & 0 & 0.75 \end{pmatrix}, \quad \boldsymbol{\Lambda}_{22} = \begin{pmatrix} 3.5 & 0 & 0 \\ 0 & 1.75 & 0 \\ 0 & 0 & 0.5 \end{pmatrix}, \quad \boldsymbol{\Lambda}_{33} = \begin{pmatrix} 2.5 & 0 & 0 \\ 0 & 2 & 0 \\ 0 & 0 & 1 \end{pmatrix}.$$

Then the auto-covariance functions are $C_{kk}(s, t) = \boldsymbol{\Phi}_k(s)^\top \boldsymbol{\Lambda}_{kk} \boldsymbol{\Phi}_k(t)$, $k = 1, 2, 3$. For the cross-covariance functions, let $C_{kk'}(s, t) = \rho \boldsymbol{\Phi}_k(s)^\top \boldsymbol{\Lambda}_{kk}^{\frac{1}{2}} \boldsymbol{\Lambda}_{k'k'}^{\frac{1}{2}} \boldsymbol{\Phi}_{k'}(t)$ for $k \neq k'$, where $\rho \in [0, 1]$ is a parameter to be specified. The induced covariance operator from the above specifications is proper; see Lemma 1 in Appendix C. Note that the absolute value of $\rho_{kk'}(s, t) = C_{kk'}(s, t) / \sqrt{C_{kk}(s, s) C_{k'k'}(t, t)}$ is bounded by ρ . Hence, ρ controls

the overall level of correlation between responses. Note also that there are 9 non-zero eigenvalues, hence, for $\ell = 1, \dots, 9$, we simulate the scores $\xi_{i\ell}$ from $\mathcal{N}(0, d_\ell)$, where d_ℓ are the induced eigenvalues. Next, we simulate the white noises $\epsilon_{ij}^{(k)}$ from $\mathcal{N}(0, \sigma_\epsilon^2)$, where $\sigma_\epsilon^2 = (2p)^{-1} \sum_\ell d_\ell$, which means that the signal-to-noise ratio is 2. The sampling time points are drawn from a uniform distribution in the unit interval and the number of observations for each subject, m_i , is generated from a uniform discrete distribution on $\{3, 4, 5, 6, 7\}$.

We use a factorial design with two factors: the number of subjects n and the correlation parameter ρ . We let $n = 100, 200$ or 400 . We let $\rho = 0.5$, which corresponds to a weak correlation between responses as the average absolute correlations between responses is only 0.36. Another value of ρ is 0.9, which corresponds to a moderate correlation between responses as the average absolute correlations between responses is about 0.50. In total, we have 6 model conditions and for each model condition we generate 200 datasets. To evaluate the prediction accuracy of the various methods, we draw 200 additional subjects as testing data.

We compare mFACES and mFPCA in terms of estimation accuracy of the covariance functions, the eigenfunctions and eigenvalues, and prediction of new subjects. For covariance function estimation, we use the relative integrated square errors (RISE). Let $\hat{C}_{kk'}(s, t)$ be an estimate of $C_{kk'}(s, t)$, then RISE are given by

$$\frac{\sum_{k=1}^p \sum_{k'=1}^p \int_0^1 \int_0^1 \{C_{kk'}(s, t) - \hat{C}_{kk'}(s, t)\}^2 ds dt}{\sum_{k=1}^p \sum_{k'=1}^p \int_0^1 \int_0^1 \{C_{kk'}(s, t)\}^2 ds dt}.$$

For estimating the ℓ th eigenfunction, we use the integrated square errors (ISE), which are defined as

$$\min \left[\sum_{k=1}^p \int_0^1 \{\Psi_\ell^{(k)}(t) - \hat{\Psi}_\ell^{(k)}(t)\}^2 dt, \sum_{k=1}^p \int_0^1 \{\Psi_\ell^{(k)}(t) + \hat{\Psi}_\ell^{(k)}(t)\}^2 dt \right].$$

Note that the range of ISE is $[0, 2]$. For estimating the eigenvalues, we use the ratio of the estimate against the truth, i.e., \hat{d}_ℓ/d_ℓ . For predicting new curves, we use the mean integrated square errors (MISE), which are given by

$$\frac{1}{200p} \sum_{k=1}^p \sum_{i=1}^{200} \left[\int_0^1 \{x_i^{(k)}(t) - \hat{x}_i^{(k)}(t)\}^2 dt \right].$$

For the curve prediction using mFPCA, we truncate the number of principal components using a PVE of 0.99. It is worth noting that if no truncation is adopted, then the curve prediction using mFPCA reduces to curve prediction using univariate FPCA. We shall also consider the conditional expectation method based on the estimates of covariance functions from mFPCA. The method is denoted by mFPCA(CE) and its difference with mFACEs is that different estimates of covariance functions are used.

3.2 Simulation Results

Figure 1 gives boxplots of RISEs of mFACEs and mFPCA for estimating covariance functions. Under all model conditions, mFACEs outperforms mFPCA and the improvement in RISEs as the sample size increases is much more pronounced for mFACEs. Under the model conditions with moderate correlations ($\rho = 0.9$), the advantage of mFACEs is substantial even for the small sample size $n = 100$.

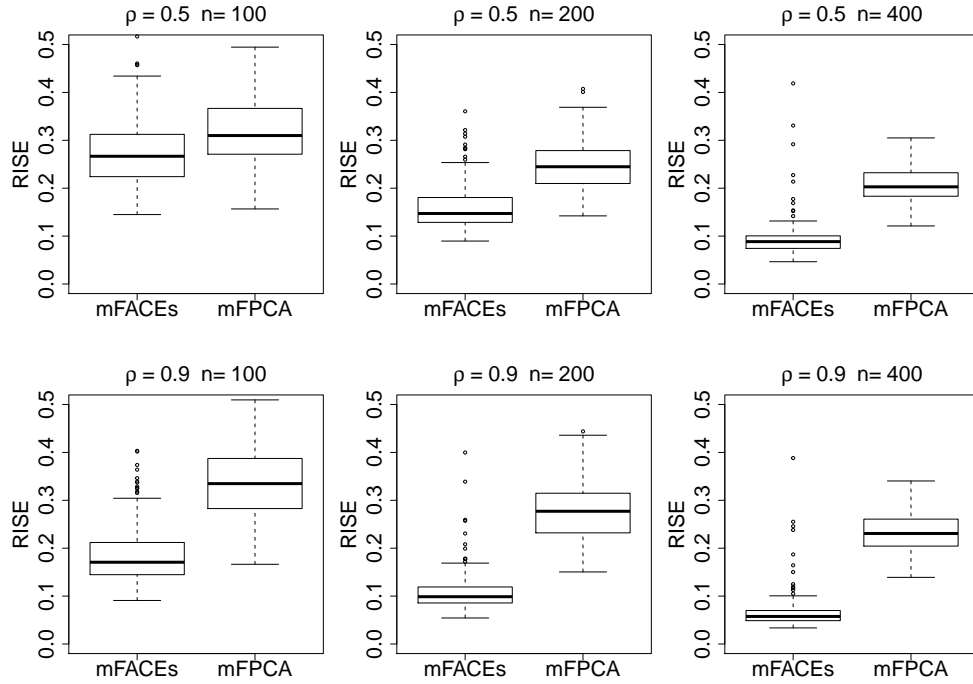


Figure 1: Boxplots of RISEs of mFACEs and mFPCA for estimating the covariance function.

Figures 2 and 3 give boxplots of ISEs and violin plots of mFACEs and mFPCA for

estimating the top two eigenfunctions and eigenvalues, respectively. Note that the top two eigenvalues account for about 60% of the total variation in the functional data for $\rho = 0.5$ and it is 80% for $\rho = 0.9$. Fig 2 shows that while the two methods are overall comparable for estimating the 1st eigenfunction, mFACES has a much better accuracy for estimating the second eigenfunction than mFPCA. The violin plots in Fig 3 shows that mFACES outperforms mFPCA substantially for estimating both eigenvalues under all model conditions. Note that the mFPCA always underestimates the eigenvalues as the biased scores from univariate FPCA underestimate the variation in functional data and hence leads to underestimates of eigenvalues.

Finally, we consider the prediction of new subjects by mFACES, mFPCA and mFPCA(CE). We define the relative efficiencies of different methods as the ratios of MISEs with respect to that of univariate FPCA; see Figure 4. Univariate FPCA is implemented in the R package `face` (Xiao et al., 016a). We have the following findings. Under all model conditions, mFACES has the smallest MISE, mFPCA(CE) has the second best performance, and mFPCA is close to univariate FPCA. Thus, on average mFACES provides the most accurate curve prediction. These results indicate that: 1) mFACES has better covariance estimation than mFPCA(CE), and so is the prediction based on it; 2) compared to mFPCA/univariate FPCA, mFPCA(CE) exploits the correlation information and hence results in better predictions.

In summary, mFACES shows competing performance against alternative methods.

4 Application to Alzheimer’s Disease Study

The Alzheimer’s Disease Neuroimaging Initiative (ADNI) is a two-stage longitudinal observational study launched in year 2003 with the primary goal of investigating whether serial neuroimags, biological markers, clinical and neuropsychological assessments can be combined to measure the progression of Alzheimer’s disease (AD) (Weiner et al., 2017). The ADNI-1 data from the first stage contain 379 patients with amnesic mild cognitive impairment (MCI, a risk state for AD) at baseline who had at least one follow-up visit. Participants were assessed at baseline, 6, 12, 18, 24, and 36 months

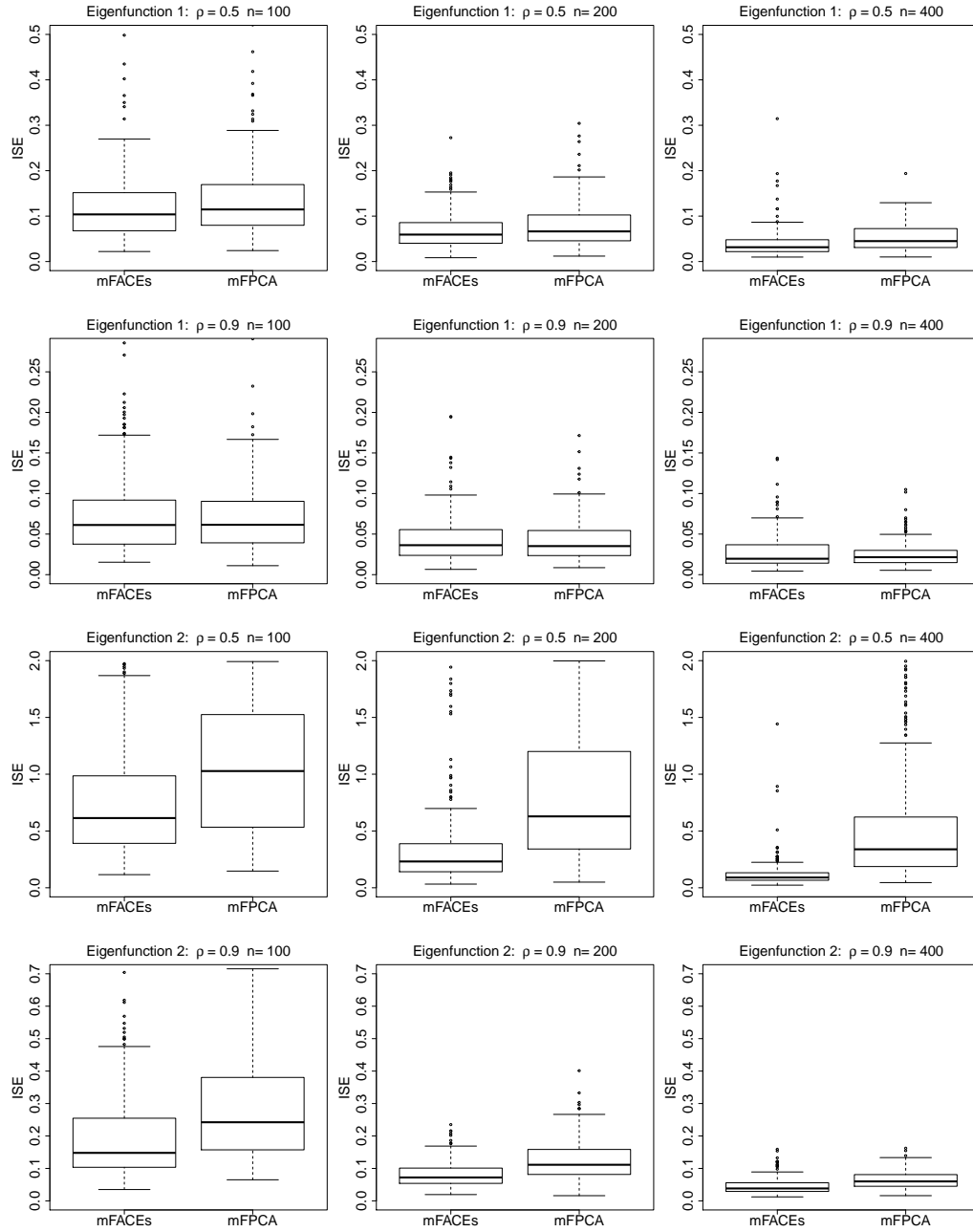


Figure 2: Boxplots of ISEs of mFACES and mFPCA for estimating the top two eigenfunctions.

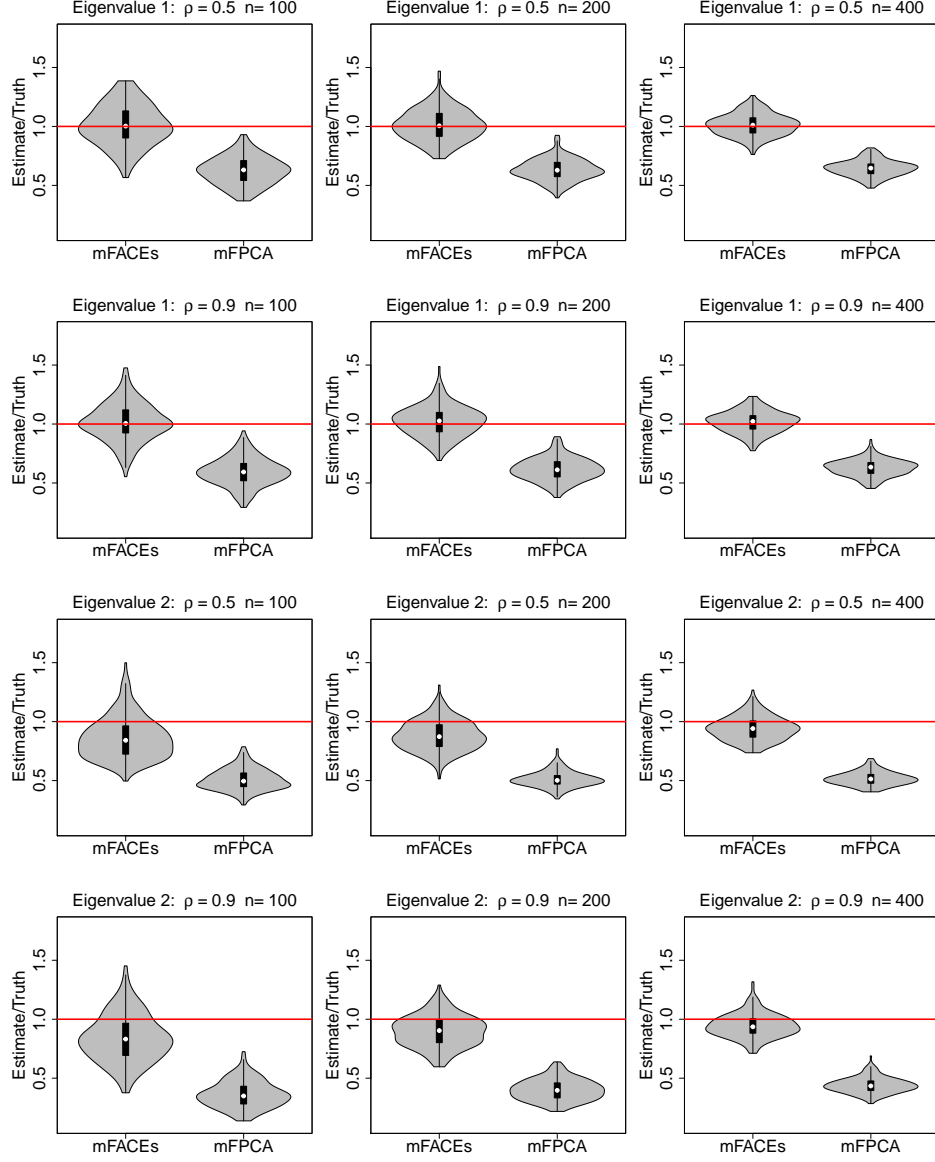


Figure 3: Violin plots of mFACES and mFPCA for estimating the top two eigenvalues.

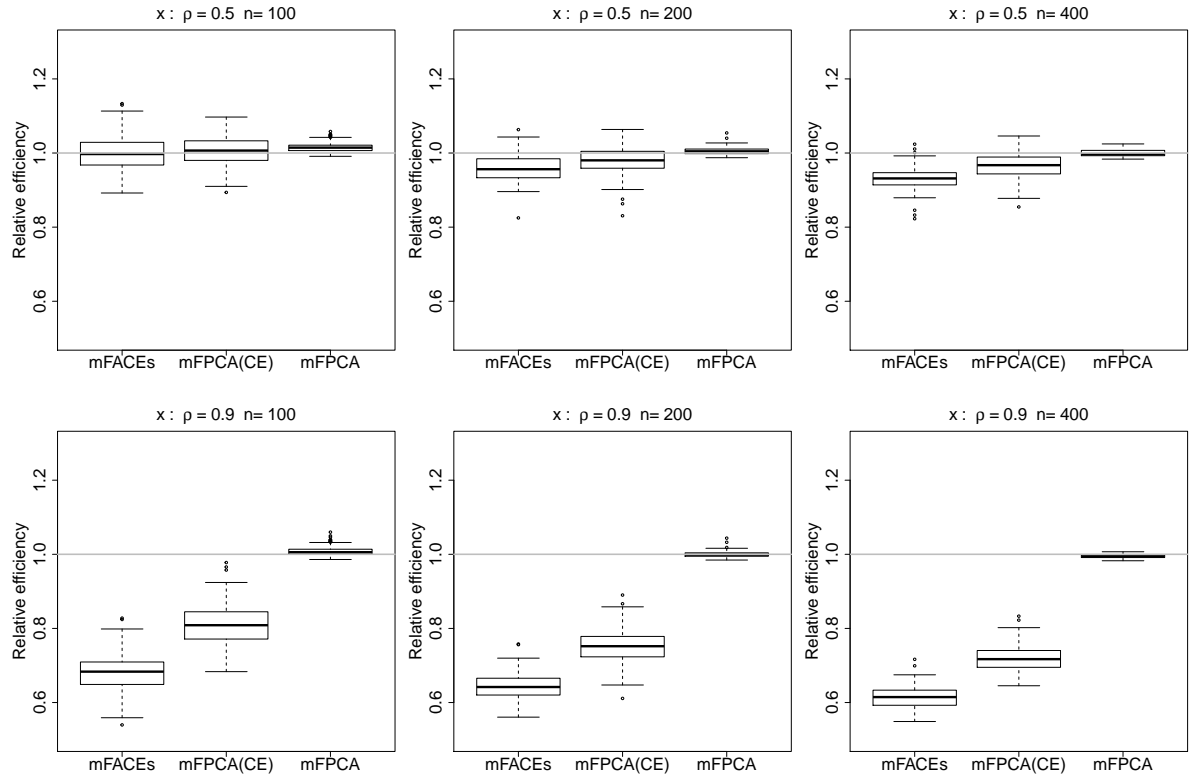


Figure 4: Boxplots of relative efficiency of three methods for curve prediction. The gray horizontal line is the MISEs for univariate FPCA.

with additional annual follow-ups included in the second stage of the study. At each visit, various neuropsychological assessments, clinical measures, and brain images were collected. The ADNI-2 data include 424 additional patients suffering from MCI and significant memory concern, with at least one follow-up visit and longitudinal data collected over four years. Thus, for the combined data, the total number of subjects is 803, and the average number of visits is 4.72. The data are publicly available at <http://ida.loni.ucla.edu/>.

We consider five longitudinal markers commonly measured in studies of AD with strong comparative predictive value (Li et al., 2017). Among the five markers, Disease Assessment Scale-Cognitive 13 items (ADAS-Cog 13), Rey Auditory Verbal Learning Test immediate recall (RAVLT.imme), Rey Auditory Verbal Learning Test learning curve (RAVLT.learn), and Mini-Mental State Examination (MMSE) are neuropsychological assessments. Functional Assessment Questionnaire (FAQ) is a functional and behavioral assessment. High values of ADAS-Cog 13 and FAQ indicate a high-risk state for AD, whereas low values of RAVLT.imme, RAVLT.learn and MMSE reflect severe cognitive impairment. The longitudinal trajectories in ADNI-1 and ADNI-2 are defined on the same time domain with the largest follow-up time 96 months from the start of ADNI-1.

4.1 Multivariate FPCA via mFACES

We analyze the data for the five longitudinal biomarkers using mFACES. For better visualization, we plot in Figure 5 the estimated correlation functions $\rho_{kk'}(s, t) = C_{kk'}(s, t) / \sqrt{C_{kk}(s, s)C_{k'k'}(t, t)}$. The plot indicates of two groups of biomarkers: ADAS-Cog 13 and FAQ in one group whereas RAVLT.imme, RAVLT.learn and NMESE in another group. The biomarkers within the groups are positively correlated and negatively correlated between groups, which make sense as high values of ADAS-Cog 13 and FAQ and low values for the other biomarkers suggest of AD. Next, we display in Figure 6 the two estimated (multivariate) eigenfunctions associated with the top two estimated eigenvalues, which account for 69% and 11% of the total variance in the functional part of the data, respectively. The eigenfunctions reveal how the 5 biomarkers

co-variate and how a subject's trajectories of biomarkers deviate from the population mean. Indeed, we see from Figure 6 that the first eigenfunction (solid curves) is below the zero-line for ADAS-Cog 13 and FAQ and above the zero-line for the other three biomarkers. This means that the score corresponding to the first eigenfunction might be used as an indicator of AD. Indeed, a negative score for the first eigenfunction means higher-than-population-mean values of the former while lower-than-population-mean values of the latter, indicating more severe AD status. The second eigenfunction (dashed curves) for the five biomarkers is below the zero line at first and then above it or the other way around, potentially suggesting of a longitudinal pattern of the AD progression. Specifically, these subjects with a positive score for the second eigenfunction will have higher ADAS-Cog 13/FAQ and lower RAVLT and MMSE over the months, suggesting of AD progression. Finally, we illustrate in Figure 7 the predicted curves along with the associated 95% point-wise confidence bands for three subjects. We focus on predicting the trajectories over the first four years as there are more observations. We can see that the confidence bands are getting wider at the later time points because of fewer observations.

4.2 Comparison of Prediction Performance of Different Methods

We compare the proposed mFACES with mFPCA and mFPCA(CE) for predicting the five longitudinal biomarkers. The prediction performance is evaluated by the average squared prediction errors (APE),

$$\text{APE}_k = \frac{1}{n} \sum_{i=1}^n \left[\frac{1}{m_i} \sum_{j=1}^{m_i} \left\{ y_{ij}^{(k)} - \hat{y}_{ij}^{(k)} \right\}^2 \right],$$

where $\hat{y}_{ij}^{(k)}$ is the predicted value of the k th biomarker for the i th subject at time t_{ij} . We conduct two types of validation: an internal validation and an external validation. For the internal validation, we perform a 10-fold cross-validation to the combined data of ADNI-1 and ADNI-2. For the external validation, we fit the model using only the ADNI-1 data and then predict ADNI-2 data. Fig 8 summarizes the results. For

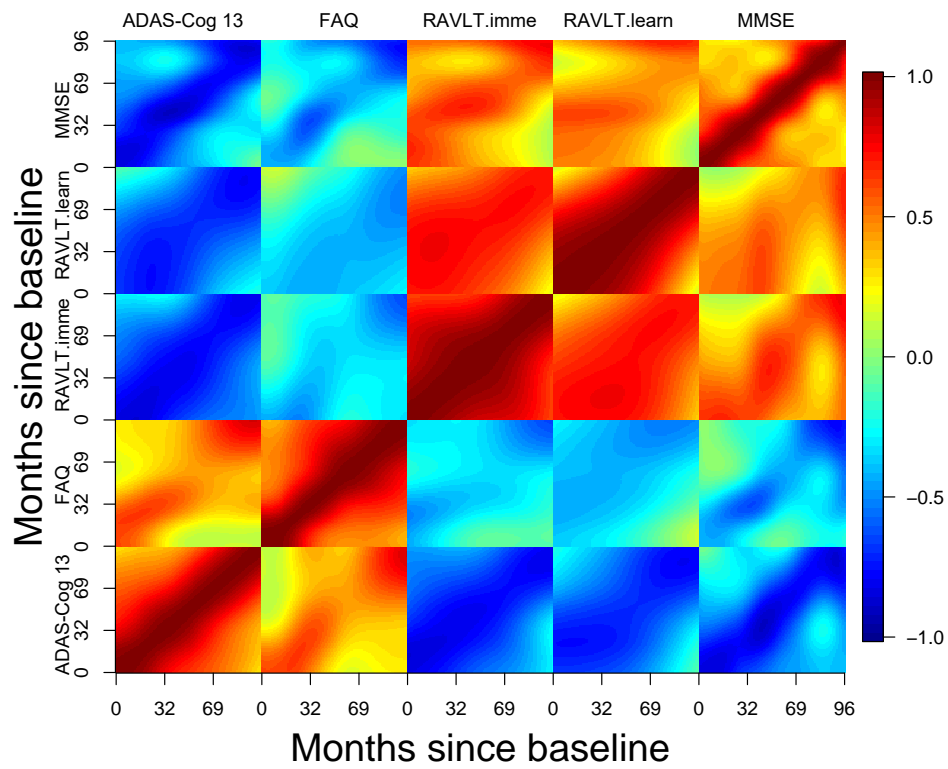


Figure 5: Estimated correlation functions for the longitudinal markers.

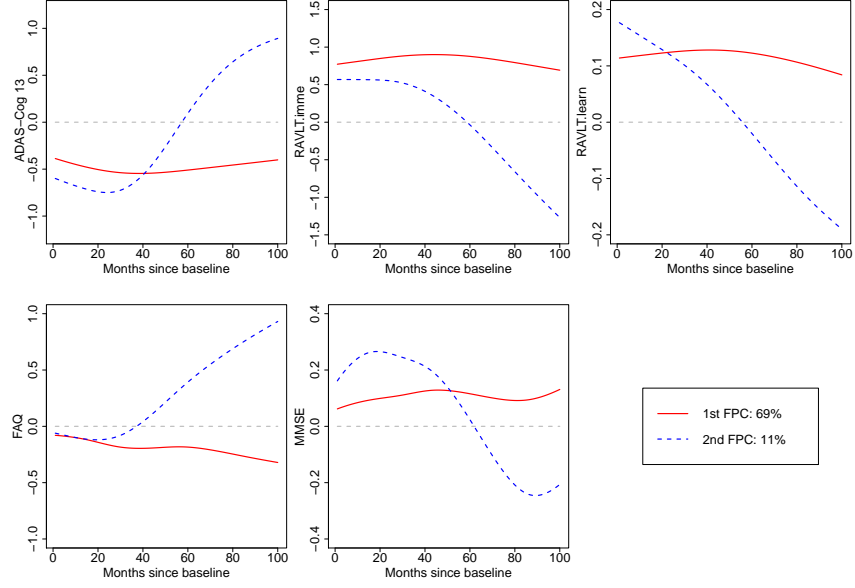


Figure 6: Estimated top two eigenfunctions for the longitudinal markers.

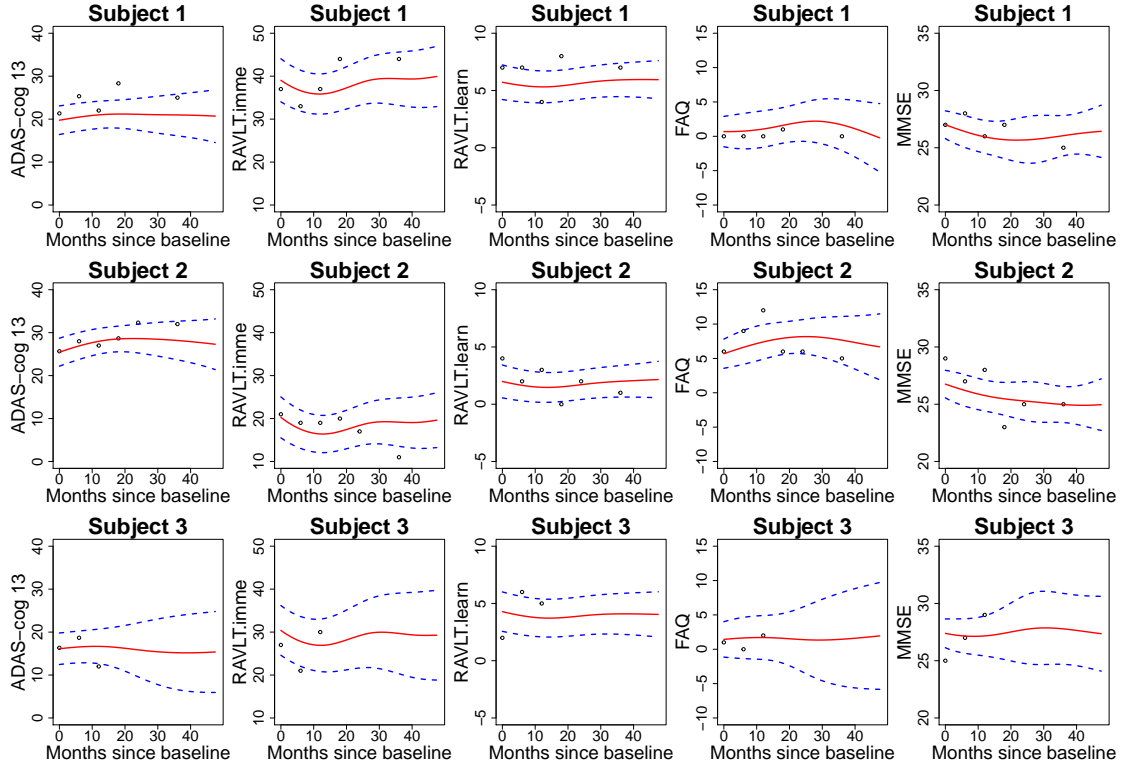


Figure 7: Predicted subject-specific curves (red solid line) of the longitudinal markers and associated 95% confidence bands (blue dotted line) for three subjects.

simplicity, we present the relative efficiency of APE, which is the ratio of APEs of one method against the mFPCA. In both cases, mFACES achieves better prediction accuracy than competing methods. Note that mFPCA(CE) outperforms mFPCA for predicting almost all biomarkers. The results suggest that: 1) mFACES is better than competing methods for analyzing the longitudinal biomarkers. 2) exploiting the correlations between the biomarkers improve prediction.

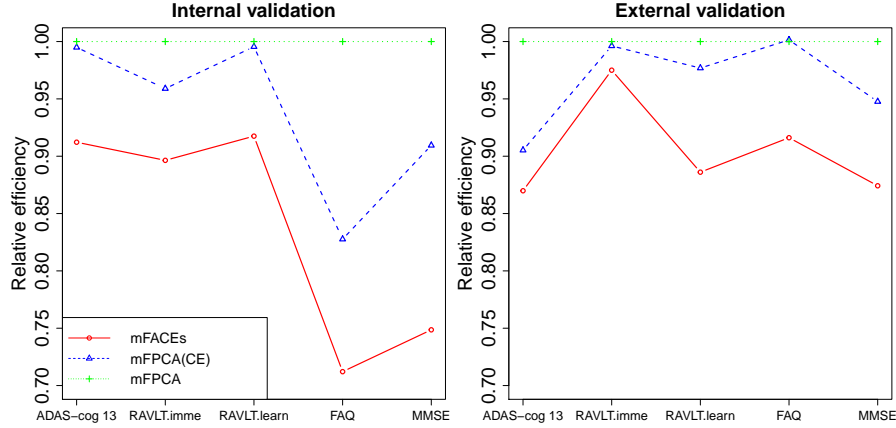


Figure 8: The internal and external prediction validations for the ADNI longitudinal makers.

5 Discussion

The prevalence of multivariate functional data has sparked much research interests in recent years. However, covariance estimation for multivariate sparse functional data remains underdeveloped. We proposed a new method, mFACES, and its features include: 1) a covariance smoothing framework is proposed to tackle multivariate sparse functional data; 2) an automatic and fast fitting algorithm is adopted to ensure the scalability of the method; 3) eigenfunctions and eigenvalues can be obtained through a one-time spectral decomposition, and eigenfunctions can be easily evaluated at any sampling points; 4) a multivariate extension of the conditional expectation approach (Yao et al., 2005) is derived to exploit correlations between outcomes. The simulation study and the data example showed that mFACES could better capture between-

function correlations and thus gave improved principal component analysis and curve prediction.

When the magnitude of functional data are quite different, one may first normalize the functional data, as recommended by Chiou et al. (2014). One method of normalization is to rescale the functional data using the estimated variance function $\widehat{C}_{kk}(t, t)^{-1/2}$ as in Chiou et al. (2014) and Jacques and Preda (2014). An alternative method is to use a global rescaling factor like $\left(\int \widehat{C}_{kk}(t, t) dt\right)^{-1/2}$ as in Happ and Greven (2017). Both methods can be easily incorporated into our proposed method. In our data analysis, we find that the results with normalization are very close to those without normalization, thus we present the results without normalization.

Because multivariate FPCA is more complex than univariate FPCA, weak correlations between the functions and small sample size may offset the benefit of conducting multivariate FPCA, see Section 7.3 in Wong et al. (2017). Thus, it is of future interest to develop practical tests to determine if correlations between multivariate functional data are different from 0.

The mFACES method has been implemented in an R package `mfaces` and will be submitted to CRAN for public access.

Appendices

Appendix A: Mean Function Estimation

The smooth mean function $\mu^{(k)}(t)$ is approximated by the B-spline basis functions $f^{(k)}(t) = \sum_{1 \leq \gamma \leq c} \alpha_\gamma^{(k)} B_\gamma(t)$, where $\boldsymbol{\alpha}_k = \left\{ \alpha_1^{(k)}, \dots, \alpha_c^{(k)} \right\}^\top \in \mathbb{R}^c$ is a coefficient vector. For simplicity, we use the same set of B-spline bases as in the covariance function estimation. We carry out univariate smoothing for each response using P -splines (Eilers and Marx, 1996) and $\boldsymbol{\alpha}_k$ is obtained by minimizing

$$\sum_{i=1}^n \sum_{j=1}^{m_i} \left\{ f^{(k)}(t_{ij}) - y_{ij}^{(k)} \right\}^2 + \tau_k \|\mathbf{D}\boldsymbol{\alpha}_k\|^2, \quad (11)$$

where τ_k is a nonnegative smoothing parameter to be selected by leave-one-subject-out cross validation for the k th response. Note that the penalty term is essentially

equivalent to the integrated squared second derivative of $f^{(k)}$. Denote the minimizer of (11) by $\hat{\alpha}_k$, then the estimate of the mean function $\mu^{(k)}(t)$ is given by $\hat{\mu}^{(k)}(t) = \sum_{1 \leq \gamma \leq c} \hat{\alpha}_\gamma^{(k)} B_\gamma(t)$.

Appendix B: Proofs of Propositions 1 and 2

Proof of Proposition 1. Define $\tilde{\mathbf{b}}(t) = \mathbf{G}^{-\frac{1}{2}} \mathbf{b}(t)$, then $\int \tilde{\mathbf{b}}(t) \tilde{\mathbf{b}}(t)^\top dt = \mathbf{I}$. Define $\check{\Theta}_{kk'}(t) = \mathbf{G}^{\frac{1}{2}} \Theta_{kk'} \mathbf{G}^{\frac{1}{2}}$. According to (1),

$$\begin{aligned} d_\ell \Psi_\ell^{(k)}(s) &= \sum_{k'=1}^p \int \mathbf{b}(s)^\top \Theta_{kk'} \mathbf{b}(t) \Psi_\ell^{(k')}(t) dt \\ &= \tilde{\mathbf{b}}(s)^\top \sum_{k'=1}^p \check{\Theta}_{kk'} \int \tilde{\mathbf{b}}(t) \Psi_\ell^{(k')}(t) dt. \end{aligned}$$

Thus, $\Psi_\ell^{(k)}(s) = \tilde{\mathbf{b}}(s)^\top \mathbf{u}_\ell^{(k)}$ with $\mathbf{u}_\ell^{(k)} = d_\ell^{-1} \left\{ \sum_{k'=1}^p \check{\Theta}_{kk'} \int \tilde{\mathbf{b}}(t) \Psi_\ell^{(k')}(t) dt \right\} \in \mathbb{R}^c$ and $\mathbf{u}_\ell = (\mathbf{u}_\ell^{(1)\top}, \dots, \mathbf{u}_\ell^{(p)\top})^\top \in \mathbb{R}^{pc}$. Since $\sum_{k=1}^p \int \Psi_\ell^{(k)}(t) \Psi_{\ell'}^{(k)}(t) dt = 1_{\{\ell=\ell'\}}$, we derive that

$$\mathbf{u}_\ell^\top \mathbf{u}_{\ell'} = \sum_{k=1}^p \mathbf{u}_\ell^{(k)\top} \mathbf{u}_{\ell'}^{(k)} = 1_{\{\ell=\ell'\}}. \quad (12)$$

By (2),

$$C_{kk'}(s, t) = \tilde{\mathbf{b}}(s)^\top \check{\Theta}_{kk'} \tilde{\mathbf{b}}(t) = \tilde{\mathbf{b}}(s)^\top \left\{ \sum_{\ell \geq 1} d_\ell \mathbf{u}_\ell^{(k)} \mathbf{u}_\ell^{(k')\top} \right\} \tilde{\mathbf{b}}(t),$$

which gives

$$\check{\Theta}_{kk'} = \sum_{\ell \geq 1} d_\ell \mathbf{u}_\ell^{(k)} \mathbf{u}_\ell^{(k')\top}.$$

As $1 \leq k, k' \leq p$, the above is equivalent to

$$\underbrace{\begin{pmatrix} \check{\Theta}_{11} & \dots & \check{\Theta}_{1p} \\ \vdots & \ddots & \vdots \\ \check{\Theta}_{p1} & \dots & \check{\Theta}_{pp} \end{pmatrix}}_{:= \check{\Theta}} = \sum_{\ell \geq 1} d_\ell \mathbf{u}_\ell \mathbf{u}_\ell^\top.$$

Because of (12), \mathbf{u}_ℓ s are orthonormal eigenvectors of $\check{\Theta}$ with d_ℓ s the corresponding eigenvalues. The proof is now complete. \square

Proof of Proposition 2. By (10),

$$\text{iGCV} = \left\| \widehat{\mathbf{C}} \right\|^2 - 2\mathbf{f}^\top \boldsymbol{\Sigma}^{-1} \mathbf{f} + \mathbf{f}^\top \boldsymbol{\Sigma}^{-2} \mathbf{f} + 2 \sum_{i=1}^n (\mathbf{L}_i \boldsymbol{\Sigma}^{-1} \mathbf{f} - \mathbf{f}_i)^\top \boldsymbol{\Sigma}^{-1} (\mathbf{L}_i \boldsymbol{\Sigma}^{-1} \mathbf{f} - \mathbf{f}_i). \quad (13)$$

Since $\boldsymbol{\Sigma}^{-1} = \mathbf{U} \text{diag}(\tilde{\mathbf{d}}) \mathbf{U}^\top$, we have

$$\mathbf{f}^\top \boldsymbol{\Sigma}^{-1} \mathbf{f} = \tilde{\mathbf{f}}^\top \text{diag}(\tilde{\mathbf{d}}) \tilde{\mathbf{f}} = \tilde{\mathbf{d}}^\top (\tilde{\mathbf{f}} \odot \tilde{\mathbf{f}}). \quad (14)$$

Similarly,

$$\mathbf{f}^\top \boldsymbol{\Sigma}^{-2} \mathbf{f} = \tilde{\mathbf{f}}^\top \text{diag}(\tilde{\mathbf{d}}^2) \tilde{\mathbf{f}} = (\tilde{\mathbf{f}} \odot \tilde{\mathbf{d}})^\top (\tilde{\mathbf{f}} \odot \tilde{\mathbf{d}}). \quad (15)$$

Next we derive that

$$\begin{aligned} & (\mathbf{L}_i \boldsymbol{\Sigma}^{-1} \mathbf{f} - \mathbf{f}_i)^\top \boldsymbol{\Sigma}^{-1} (\mathbf{L}_i \boldsymbol{\Sigma}^{-1} \mathbf{f} - \mathbf{f}_i) \\ &= \left(\mathbf{U}^\top \mathbf{L}_i \boldsymbol{\Sigma}^{-1} \mathbf{f} - \mathbf{U}^\top \mathbf{f}_i \right)^\top \text{diag}(\tilde{\mathbf{d}}) \left(\mathbf{U}^\top \mathbf{L}_i \boldsymbol{\Sigma}^{-1} \mathbf{f} - \mathbf{U}^\top \mathbf{f}_i \right) \\ &= \left(\tilde{\mathbf{L}}_i \text{diag}(\tilde{\mathbf{d}}) \tilde{\mathbf{f}} - \tilde{\mathbf{f}}_i \right)^\top \text{diag}(\tilde{\mathbf{d}}) \left(\tilde{\mathbf{L}}_i \text{diag}(\tilde{\mathbf{d}}) \tilde{\mathbf{f}} - \tilde{\mathbf{f}}_i \right). \end{aligned}$$

It follows that

$$\begin{aligned} & (\mathbf{L}_i \boldsymbol{\Sigma}^{-1} \mathbf{f} - \mathbf{f}_i)^\top \boldsymbol{\Sigma}^{-1} (\mathbf{L}_i \boldsymbol{\Sigma}^{-1} \mathbf{f} - \mathbf{f}_i) \\ &= \tilde{\mathbf{d}}^\top \left[\left\{ \tilde{\mathbf{L}}_i (\tilde{\mathbf{f}} \odot \tilde{\mathbf{d}}) \right\} \odot \left\{ \tilde{\mathbf{L}}_i (\tilde{\mathbf{f}} \odot \tilde{\mathbf{d}}) \right\} + (\tilde{\mathbf{f}}_i \odot \tilde{\mathbf{f}}_i) \right] - 2\tilde{\mathbf{d}}^\top \left\{ (\tilde{\mathbf{f}}_i \tilde{\mathbf{f}}^\top) \odot \tilde{\mathbf{L}}_i \right\} \tilde{\mathbf{d}}. \end{aligned} \quad (16)$$

Combining (13), (14), (15) and (16), the proof is complete. \square

Appendix C: A Lemma

Lemma 1. *The covariance operator with the covariance functions defined in Section 4.1 is positive semi-definite.*

Proof. Let $\mathbf{a} = (a_1, \dots, a_p)^\top \in \mathbb{R}^p$ and $\tilde{X} = \mathbf{a}^\top \mathbf{x}$, then \tilde{X} is a stochastic process with covariance function

$$\text{Cov} \left\{ \tilde{X}(s), \tilde{X}(t) \right\} = \sum_{kk'} a_k a_{k'} C_{kk'}(s, t) = \sum_{kk'} a_k a_{k'} (\rho + (1 - \rho) 1_{\{k=k'\}}) \tilde{\boldsymbol{\Phi}}_k(s)^\top \tilde{\boldsymbol{\Phi}}_{k'}(t),$$

where $\tilde{\boldsymbol{\Phi}}_k(s) = \boldsymbol{\Phi}_k(s)^\top \boldsymbol{\Lambda}_{kk}^{\frac{1}{2}}$. Let $\boldsymbol{\Psi}(s) = \sum_{k=1}^p a_k \tilde{\boldsymbol{\Phi}}_k(s)$. Then

$$\text{Cov} \left\{ \tilde{X}(s), \tilde{X}(t) \right\} = \rho \boldsymbol{\Psi}(s)^\top \boldsymbol{\Psi}(t) + (1 - \rho) \sum_k a_k^2 \tilde{\boldsymbol{\Phi}}_k(s)^\top \tilde{\boldsymbol{\Phi}}_k(t).$$

which is always positive semi-definite and the proof is complete. \square

SUPPLEMENTARY MATERIAL

Supplement: Additional results of a simulation which mimics the ADNI data. (<http://www4.ncsu.edu/~cli9/mFACEs/supplement.pdf>)

mfaces R package: R package `mfaces` containing an open source implementation of the proposed method described in the article. (Available upon request)

Demo code: Code to demonstrate the proposed method with a simulated dataset in Section 3. (Available upon request)

References

- Berrendero, J., A. Justel, and M. Svarc (2011). Principal components for multivariate functional data. *Computational Statistics & Data Analysis* 55(9), 2619–2634.
- Cai, T. and M. Yuan (2010). Nonparametric covariance function estimation for functional and longitudinal data. *University of Pennsylvania and Georgia institute of technology*.
- Chiou, J.-M., Y.-T. Chen, and Y.-F. Yang (2014). Multivariate functional principal component analysis: A normalization approach. *Statistica Sinica*, 1571–1596.
- Chiou, J.-M. and H.-G. Müller (2014). Linear manifold modelling of multivariate functional data. *Journal of the Royal Statistical Society: Series B (Statistical Methodology)* 76(3), 605–626.
- Chiou, J.-M. and H.-G. Müller (2016). A pairwise interaction model for multivariate functional and longitudinal data. *Biometrika* 103(2), 377–396.
- Eilers, P. and B. Marx (1996). Flexible smoothing with B-splines and penalties (with Discussion). *Statist. Sci.* 11, 89–121.
- Eilers, P. and B. Marx (2003). Multivariate calibration with temperature interaction using two-dimensional penalized signal regression. *Chemometrics and Intelligent Laboratory Systems* 66, 159–174.
- Goldsmith, J., C. Crainiceanu, B. Caffo, and D. Reich (2012). Longitudinal penalized functional regression for cognitive outcomes on neuronal tract measurements. *Journal of the Royal Statistical Society: Series C (Applied Statistics)* 61, 453–469.
- Greven, S., C. Crainiceanu, B. Caffo, and D. Reich (2010). Longitudinal functional principal component. *Electronic J. Statist.* 4, 1022–1054.
- Happ, C. and S. Greven (2017). Multivariate functional principal component analysis for data observed on different (dimensional) domains. *Journal of the American Statistical Association* (just-accepted).

- Huang, H., Y. Li, and Y. Guan (2014). Joint modeling and clustering paired generalized longitudinal trajectories with application to cocaine abuse treatment data. *Journal of the American Statistical Association* 109(508), 1412–1424.
- Jacques, J. and C. Preda (2014). Model-based clustering for multivariate functional data. *Computational Statistics & Data Analysis* 71, 92–106.
- James, G., T. Hastie, and C. Sugar (2000). Principal component models for sparse functional data. *Biometrika* 87, 587–602.
- Kowal, D. R., D. S. Matteson, and D. Ruppert (2017). A bayesian multivariate functional dynamic linear model. *Journal of the American Statistical Association* 112(518), 733–744.
- Leng, X. and H. Müller (2006). Classification using functional data analysis for temporal gene expression data. *Bioinformatics* 22, 68–76.
- Li, J., C. Huang, H. Zhu, and A. D. N. Initiative (2017). A functional varying-coefficient single-index model for functional response data. *Journal of the American Statistical Association* 112(519), 1169–1181.
- Li, K., W. Chan, R. S. Doody, J. Quinn, and S. Luo (2017). Prediction of conversion to alzheimers disease with longitudinal measures and time-to-event data. *Journal of Alzheimer’s Disease* 58(2), 361–371.
- Li, Y., N. Wang, and R. J. Carroll (2013). Selecting the number of principal components in functional data. *Journal of the American Statistical Association* 108(504), 1284–1294.
- Lindquist, M. (2012). Functional causal mediation analysis with an application to brain connectivity. *Journal of the American Statistical Association* 107, 1297–1309.
- Luo, R. and X. Qi (2017). Function-on-function linear regression by signal compression. *Journal of the American Statistical Association* 112(518), 690–705.

- Morris, J., C. Arroyo, B. Coull, L. Ryan, R. Herrick, and S. Gortmaker (2006). Using wavelet-based functional mixed models to characterize population heterogeneity in accelerometer profiles: A case study. *Journal of the American Statistical Association* 101, 1352–1364.
- Park, J. and J. Ahn (2017). Clustering multivariate functional data with phase variation. *Biometrics* 73(1), 324–333.
- Peng, J. and D. Paul (2009). A geometric approach to maximum likelihood estimation of functional principal components from sparse longitudinal data. *J. Comput. Graph. Stat.* 18, 995–1015.
- Petersen, A. and H.-G. Müller (2016). Fréchet integration and adaptive metric selection for interpretable covariances of multivariate functional data. *Biometrika* 103(1), 103–120.
- Qi, X. and R. Luo (2018). Function-on-function regression with thousands of predictive curves. *Journal of Multivariate Analysis* 163, 51–66.
- Qiao, X., S. Guo, and G. M. James (2017). Functional graphical models. *Journal of the American Statistical Association* (just-accepted).
- Ramsay, J. and B. Silverman (2005). *Functional data analysis*. New York: Springer.
- Reimherr, M. and D. Nicolae (2014). A functional data analysis approach for genetic association studies. *The Annals of Applied Statistics* 8, 406–429.
- Reimherr, M. and D. Nicolae (2016). Estimating variance components in functional linear models with applications to genetic heritability. *Journal of the American Statistical Association* 111, 407–422.
- Reiss, P. and R. Ogden (2010). Functional generalized linear models with images as predictors. *Biometrics* 66, 61–69.
- Saporta, G. (1981). Méthodes exploratoires danalyse de données temporelles. *Cahiers du bureau universitaire de recherche opérationnelle* (37-38).

- Seber, G. (2007). *A Matrix Handbook for Statisticians*. New Jersey: Wiley-Interscience.
- Weiner, M. W., D. P. Veitch, P. S. Aisen, L. A. Beckett, N. J. Cairns, R. C. Green, D. Harvey, C. R. Jack, W. Jagust, J. C. Morris, et al. (2017). Recent publications from the alzheimer’s disease neuroimaging initiative: Reviewing progress toward improved ad clinical trials. *Alzheimer’s & dementia: the journal of the Alzheimer’s Association* 13(4), e1–e85.
- Wong, R. K., Y. Li, and Z. Zhu (2017). Partially linear functional additive models for multivariate functional data. *Journal of the American Statistical Association* (just-accepted).
- Wood, S. N. (2000). Modelling and smoothing parameter estimation with multiple quadratic penalties. *Journal of the Royal Statistical Society: Series B (Statistical Methodology)* 62(2), 413–428.
- Xiao, L., L. Huang, J. Schrack, L. Ferrucci, V. Zipunnikov, and C. Crainiceanu (2015). Quantifying the life-time circadian rhythm of physical activity: a covariate-dependent functional approach. *Biostatistics* 16, 352–367.
- Xiao, L., C. Li, W. Checkley, and C. Crainiceanu (2016a). R package *face*: Fast covariance estimation for sparse functional data (version 0.1-4). URL:<http://cran.r-project.org/web/packages/face/index.html>.
- Xiao, L., C. Li, W. Checkley, and C. Crainiceanu (2018). Fast covariance estimation for sparse functional data. *Statistics and Computing* 28, 511–522.
- Xu, G. and J. Huang (2012). Asymptotic optimality and efficient computation of the leave-subject-out cross-validation. *Ann. Statist.* 40, 3003–3030.
- Yao, F., H. Müller, and J. Wang (2005). Functional data analysis for sparse longitudinal data. *J. Amer. Statist. Assoc.* 100, 577–590.
- Zhou, L., J. Z. Huang, and R. J. Carroll (2008). Joint modelling of paired sparse functional data using principal components. *Biometrika* 95(3), 601–619.

- Zhou, S., X. Shen, D. Wolfe, et al. (1998). Local asymptotics for regression splines and confidence regions. *The annals of statistics* 26(5), 1760–1782.
- Zhu, H., P. Brown, and J. Morris (2012). Robust classification of functional and quantitative image data using functional mixed models. *Biometrics* 68, 1260–1268.
- Zhu, H., R. Li, and L. Kong (2012). Multivariate varying coefficient model for functional responses. *Annals of statistics* 40(5), 2634.
- Zhu, H., J. S. Morris, F. Wei, and D. D. Cox (2017). Multivariate functional response regression, with application to fluorescence spectroscopy in a cervical pre-cancer study. *Computational statistics & data analysis* 111, 88–101.
- Zhu, H., N. Strawn, and D. B. Dunson (2016). Bayesian graphical models for multivariate functional data. *Journal of Machine Learning Research* 17(204), 1–27.